Compound events in Germany in 2018: drivers and case studies

Elena Xoplaki[1,2], Florian Ellsäßer[2,a], Jens Grieger[3], Katrin M. Nissen[3], Joaquim G. Pinto[4], Markus Augenstein[4], Ting-Chen Chen[4], Hendrik Feldmann[4], Petra Friederichs[5], Daniel Gliksman[6,7], Laura Goulier[8], Karsten Haustein[9,b], Jens Heinke[10], Lisa Jach[11], Florian Knutzen[9], Stefan Kollet[8], Jürg Luterbacher[1,2], Niklas Luther[2], Susanna Mohr[4,12], Christoph Mudersbach[13], Christoph Müller[10], Efi Rousi[14], Felix Simon[13], Laura Suarez-Gutierrez[15,c,d], Svenja Szemkus[5], Sara M. Vallejo-Bernal[16,17], Odysseas Vlachopoulos[2], Frederik Wolf[16]

[1] Department of Geography, Climatology, Climate Dynamics and Climate Change, Justus Liebig University Giessen, Giessen, Germany
[2] Centre of International Development and Environmental Research, Justus Liebig University Giessen, Giessen, Germany
[3] Institute of Meteorology, Free University of Berlin, Berlin, Germany
[4] Institute of Meteorology and Climate Research (IMK-TRO), Karlsruhe Institute of Technology (KIT), Karlsruhe, Germany
[5] Institute of Geosciences, University of Bonn, Bonn, Germany
[6] Institute of Hydrology and Meteorology, Faculty of Environmental Sciences, Dresden University of Technology, Tharandt, Germany
[7] Institute of Geography, Dresden University of Technology, Dresden, Germany
[8] Institute for Bio- and Geosciences, Research Centre Jülich, Jülich, Germany
[9] Climate Service Center Germany (GERICS), Helmholtz-Zentrum Hereon, Hamburg, Germany
[10] Potsdam Institute for Climate Impact Research (PIK), Member of the Leibniz Association, Potsdam, Germany
[11] Institute of Physics and Meteorology, University of Hohenheim, Stuttgart, Germany
[12] Center for Disaster Management and Risk Reduction Technology (CEDIM), Karlsruhe Institute of Technology, Karlsruhe, Germany
[13] Department of Hydraulic Engineering and Hydromechanics, Civil and Environmental Engineering, Bochum University of Applied Sciences, Bochum, Germany
[14] Potsdam Institute for Climate Impact Research (PIK), Member of the Leibniz Association, Potsdam, Germany
[15] Max-Planck-Institut für Meteorologie, Hamburg, Germany
[16] Research Department IV - Complexity Science, Potsdam Institute for Climate Impact Research (PIK), Member of the Leibniz Association, Potsdam, Germany
[17] Institute of Geosciences, University of Potsdam, Potsdam, Germany
[a] now at: Department of Natural Resources, ITC - Faculty of Geoinformation Science and Earth Observation, University of Twente, The Netherlands
[b] now at: Institute for Meteorology, University of Leipzig, Leipzig, Germany
[c] now at: Institute for Atmospheric and Climate Science, ETH Zurich, Zurich, Switzerland
[d] now at: Institut Pierre-Simon Laplace, CNRS, Paris, France

Correspondence to: Elena Xoplaki (elena.xoplaki@geogr.uni-giessen.de)

Abstract. Europe frequently experiences by a wide range of extreme events and natural hazards, including heatwaves, extreme precipitation, droughts, cold spells, windstorms, and storm surges. Many of these events do not occur as single extreme events, but rather show a multivariate character, known as compound events. We investigate the interactions between extreme weather events, their characteristics, changes in intensity, frequency, as well as uncertainties in the past, present and future. We also explore their impacts on various socio-economic sectors in Germany and Central Europe. This contribution highlights several

case studies with special focus on 2018, a year marked by an exceptional sequence of compound events across large parts of Europe, resulting in severe impacts on human lives, ecosystems, and infrastructure. We provide new insights into the drivers of spatially and temporally compound events, such as heat and drought and heavy precipitation combined with extreme winds, and their adverse effects on ecosystems and society, using large-scale atmospheric patterns. We also examine the interannual influence of droughts on surface water, and the impact of water scarcity and heatwaves on agriculture and forests. we assess projected changes in compound events at different current and future global surface temperature levels, demonstrating the need for improved quantification of future extreme events to support adaptation planning. Finally, we address research gaps and future directions, stressing the importance of defining composite events primarily in terms of their impacts prior to their statistical characterisation.

1 Introduction

Extreme temperatures, strong extratropical low pressure systems and their associated extreme winds and heavy precipitation events can have devastating socio-economic impacts. Moreover, the combination of otherwise regular climate and weather phenomena can unfold their effects beyond the individual events (Ridder et al., 2020) and have devastating consequences and impacts (Ridder et al., 2022; Bevacqua et. al., 2017, 2021, 2023 and references therein). Thus, human and natural systems that are usually able to handle the impacts of single extreme events are challenged by the co-occurrence of two or more extremes (compound events, CE) which severely increase the risk of loss and damage (Toreti et al., 2019a). Events with additive and multiplicative effects are of utmost importance and can result from mutually reinforcing cycles/positive feedback between individual events. Interrelated events, e.g., through land surface-atmosphere interactions or atmospheric moisture conditions, modify extreme events (Wang et al., 2022). The effects may develop also through atmospheric dynamics that connect features such as the 2010 Russian heatwave and the flood in Pakistan (Barriopedro et al., 2011; Lau et al., 2012; Zscheischler et al., 2018) or through induced responses at distant areas of significant impact to the global system (Vogel et al., 2019).

The Intergovernmental Panel on Climate Change (IPCC; Seneviratne et al., 2012) defines CEs as 1) two or more extreme events occurring simultaneously or successively, 2) a combination of extreme events with underlying conditions that amplify the impact of the events, or 3) a combination of events that are not themselves extremes but lead to an extreme event or impact when combined. This definition is embedded within the IPCC risk framework under the umbrella of a combination of multiple drivers and/or hazards that contribute to societal or environmental risks. Also embedded in this framework is the understanding that response to an imminent risk can, in its own right, serve to reduce or to increase future risks. CEs often lead to disproportionate impacts on people and ecosystems (Seneviratne et al., 2012; Leonard et al., 2014; Caldeira et al., 2015; Bastos et al., 2021). To quantify the probability of CEs in today's and future climate is of great importance specifically for adaptation planning for various sectors including agriculture, fisheries, river transport, energy supply, tourism, etc. (Zscheischler and Fischer, 2020). Recently, Zscheischler et al. (2020) extended the definition and classified CEs into 1) preconditioned events,

where a weather-driven or climate-driven precondition aggravates the impacts of a climatic impact-driver; 2) multivariate events, where multiple drivers and/or climatic impact-drivers lead to an impact; 3) temporally compounding events, where a succession of hazards leads to an impact; and 4) spatially compounding events, where hazards in multiple connected locations cause an aggregated impact. Drivers include processes, variables, and phenomena in the climate and weather domain that may span over multiple spatial and temporal scales (Zscheischler et al., 2020). Current research on weather and climate impacts, risks and damages often underestimates the influence of CEs (Ridder et al., 2021). It is therefore essential to adapt research strategies and tools, such as models, to integrate compound weather and climate events, enabling a more accurate assessment of uncertainties, impacts and risks. Further, anthropogenic climate change is expected to influence the frequency and intensity of CEs, and thus future planning for such changes requires reliable climate models, which can represent these hazards, their underlying drivers as well as their combinations. Despite this importance, studies evaluating climate model representation of CEs are still rare (Aalbers et al., 2013; Bevacqua et al., 2023; Manning et al., 2023). Further, the impact of climate change to dynamic changes in the atmosphere and consequently to the location and magnitude of extreme events and its compounds is less well understood and thus characterised as low confidence by the IPCC (IPCC, 2021). This holds true also for CEs, which are naturally even more complex due to their multivariate character, also in terms of the complexity of the atmospheric circulation state. For instance, the COVID-19 pandemic has brought dynamics of compound hazards and risk-response feedback to the forefront of hydrometeorological hazard response and preparedness (Simpson et al., 2021; Zaitchik et al., 2022). Compound hazards are rare, and those for instance that involve a disease such as COVID-19 have no recent precedent. The more complex CEs become, the clearer are the limitations of the conventional statistical approaches to risk assessment (Zaichik et al., 2022).

The development of integrated research on CEs is the objective of the European COST Action DAMOCLES (http://www.damocles.compoundevents.org) that bundled research efforts in this field, and towards which several of the authors actively contribute. One of the main knowledge gaps identified concerns how the compound character of events is changing in a warming world and will continue to change during future decades. The question on how and why extreme weather events affecting specifically Germany and Central Europe may change in a warming climate is the major topic of the climXtreme project (https://climxtreme.net/), in the frame of which this work has been conducted, aiming to analyze and understand the dynamics of extreme climate events, their impacts, and potential future trends in a changing climate. To analyse hot and dry compounds, a variety of research questions and approaches are explored: at the global scale, the precursors of spatially and temporally CEs are analysed using large-scale atmospheric patterns and jet stream states. At the European scale, the detection and identification of events and the spatial representation of key climate variables in relation to heatwaves are investigated. Focusing on Germany, the interannual influence of droughts on surface water is analysed and the impact of water scarcity and heatwaves on agriculture and forests is studied. Further, the CEs including precipitation and/or wind as a hazard are analysed focusing on a series of windstorms and convective storms with adverse impacts on ecosystems and society.

All case studies presented in this paper are selected from the calendar year 2018, which is of particular interest given the prolonged and persistent dry and hot conditions across large parts of Europe as well as featured storms Eleanor and David

(coined Burglind and Friederike in Germany and hereafter) in January 2018 and several weeks of thunderstorm activity in May and June. 2018 was also characterized by strong wind gusts that co-occurred with heavy snowfall during the windstorm Friederike (Vautard et al., 2019), a relatively dry spring with exceptionally high temperatures followed by an extremely dry summer with very warm mean temperatures over large areas of Europe (Munich Re, 2019; Zscheischler and Fischer, 2020). Total precipitation in central Europe was at the lowest percentiles relative to the 1976–2005 distribution; Germany experienced a reduction of precipitation of ~53% in July and of ~46% in August compared to the period 1981-2010 (Deutscher Wetterdienst, 2018). The summer in Germany was characterised by the most extreme combination of high temperatures, as one of the warmest years on record (Kaspar et al., 2023) and low precipitation since 1881 (Zscheischler and Fischer, 2020). The combination of the individual events caused tremendous adverse and detrimental impacts in larger areas of western Europe with a peak over Germany and on a variety of sectors ranging from agriculture and society (Manning et al., 2018; Toreti et al., 2019b; Zscheischler and Fischer, 2020; Conradt et al., 2023; Shyrokaya et al., 2024), forests (Bastos et al., 2020; Buras et al., 2020; de Brito et al., 2020; Senf and Seidl, 2021), fires (Munich Re 2019; Bastos et al., 2020), ecology (Bastos et al., 2021), soil and surface water (Liu et al., 2020; Brakkee et al., 2022; Hartick et al., 2021), marine environment (Kaiser et al., 2023), traffic disruption, power outages, property damage by e.g. falling trees, fatalities (Vautard et al., 2019) as well as human health (Matzarakis et al., 2020; Conradt et al., 2023). The exceptional heatwave of 2018 also caused many nuclear power plants to shut down because the rivers could not provide sufficient cooling capacity for the reactors (Vogel et al., 2019). In addition, Blauhut et al. (2022) surveyed stakeholders across Europe regarding their perceptions of the 2018–2019 drought and drought risk management in their respective countries. Germany was identified as being aware of drought risks but among the least prepared, lacking a formal management plan.

We study this exceptional year and the series of extremes and CEs in a sequence of the large scale, their detection and spatial representation as well as the long term impacts on soil moisture both at the continental scale and the consequent agriculture and forestry impacts at the national scale. The paper first outlines the data and methodologies used for analysing the selected CEs in 2018, followed by a detailed analysis of each case study. These case studies are categorized into temperature-precipitation and precipitation-wind CE storylines, along with an evaluation of their impacts in Germany.

2 Data and Methods

Different methodological approaches have been used, tailored to the different types of CEs, ranging from better understanding of the selected event drivers to sectoral impact assessments. This section summarizes these approaches and provides a basis for the study and analysis of the selected case studies separated in temperature-precipitation and precipitation-wind CEs. The temperature-precipitation storyline includes analysis on drivers of the hot summer of 2018, detection of extreme events and spatial patterns, assessment of the impact of the 2018 European drought on soil moisture and groundwater as well as sectoral impacts on agriculture and forestry. The storyline is complemented with an assessment of model simulations to realistically represent conditions as those of 2018 in Germany. The precipitation-wind storyline comprises the analysis of intense low

pressure systems in winter 2018, their life cycle and triggering role for compound precipitation and wind events, as well as severe convective storms during the 2018 warm season. Considering the nature of the various case studies and events during the warm season of 2018, and given the focus on compound events in this study, we aim to define the characteristics of the events analysed and their interrelationships. Additionally, a range of relative thresholds, such as the 90th, 95th, and 98th percentiles, appropriate for each variable and elaborated impact are used to define extremes, and we will provide explanations for their application.

2.1 Drivers of the hot summer of 2018

To better understand the drivers of the hot summer of 2018, Rousi et al. (2022) identified jet states in the zonal mean zonal wind over the Eurasian sector at different pressure levels for the summer months in ERA5 data (Hersbach et al., 2020) using Self-Organizing Maps (SOMs, see Kohonen, 2013; Rousi et al., 2015). A comparative approach with different cluster numbers, clustering algorithms and initializations of SOMs led to a robust cluster of double jet states. Increased persistence of those jet states was connected to heatwave events (defined as a period of at least 3 consecutive days of daily maximum temperature threshold exceedance > 90th percentile, following Fischer and Schär (2010) and a spatial extent over 40.000 km^2 within a 4° x 4° spatial sliding window, similar to Stefanon et al. (2012) across western Europe (Rousi et al., 2022).

2.2 Detection of spatial patterns of extreme events

The analysis of the large-scale temperature and precipitation deficit patterns and their expression during the 2018 heatwave at the European scale is based on the cross-Tail Pairwise Dependence Matrix (cross-TPDM) and Extreme Pattern Index (EPI) proposed by Szemkus and Friederichs (2024). Typical spatial patterns of common extremes are derived by singular value decomposition of the cross-TPDM. The cross-TPDM is a measurement of extremal dependence, rooted in extreme value theory and has comparable statistical properties to the cross-covariance matrix (Szemkus and Friederichs, 2024; Cooley an Thibaud, 2019). The singular vectors of cross-TPDM represent pairs of spatial patterns in which extremes in two variables are likely to occur simultaneously. Consequently, the expansion coefficients provide a time series for each singular vector that summarise the occurrence of extreme events within the respective pattern. The first 10 left and right expansion coefficients are then summarised in the EPI that is high when individual patterns or a linear combination of leading patterns are particularly strongly pronounced. This pattern-based analysis thus provides a robust measurement for the heatwave and drought intensity over Europe. Before calculating the cross-TPDM and EPI, the ERA5 daily 2m temperature and precipitation deficits for the summer months (June-August) of 2018 are standardised and the annual cycle is removed. Precipitation deficits are calculated as the inverse of the 90-day accumulated precipitation.

2.3 Surface water storage of the dry summer of 2018

To analyse the drought characteristics of the summer of 2018, an ensemble of simulations for the hydrological year 2018/19 is used (Hartick et al., 2021). The hydrological year 2018/2019 was initialised with land surface and subsurface conditions from the end of the hydrological year 2018 and simulated using different atmospheric boundary conditions. The proposed approach investigates the impact of hydrologic initialization, and soil and groundwater memory on water storage anomalies against the background of atmospheric variability and uncertainty on an interannual time scale. The varying atmospheric initial conditions were derived from the ERA-Interim data for each individual year between 1996 and 2018 and resulted in 22 realisations as the number of individual years within that period. Thus, the ensemble of realisations of the hydrological year 2018/2019 accounts for a large part of the atmospheric uncertainty. The analysis was performed for 20 European river basins. The 2018 drought was defined as the driest 10% of the total water storage anomalies (S) occurring in 2018 within the climatological time series. Surface water availability for the 2018/2019 hydrological year was represented by surface water storage (S_u), categorised into dry, $S_{u,d}$, and wet, $S_{u,w}$, anomalies. To ensure that an increased probability of $S_{u,d}$ in the hydrological year 2018/2019 was outside of regular climate variability, we compared the $S_{u,d}$ probability distribution of the described hydrological year 2018/2019 ensemble (Case A) with the probability distribution of $S_{u,d}$ within the climatological time series (Case B), see also the corresponding section below. Two beta distributions were generated, one for each case, by applying a prior with no information. We sampled each beta distribution 10,000 times and calculated the probability of Case A > Case B to determine the confidence that the probability of a $S_{u,d}$ after a drought is greater than the climatological variability. In addition, we obtained the uncertainty of the confidence intervals by bootstrapping 1000 times over the climatological time series. The methodology provides a probabilistic insight into the impact of a groundwater drought on future surface water resources on an interannual time scale.

2.4 Soil moisture of the dry summer of 2018

In addition to the dry surface water anomaly in Central Europe, soils showed moisture deficits (Liu et al., 2020; Bastos et al., 2020; Rousi et al., 2023; Conradt et al., 2023). This likely caused low groundwater levels (Brauns et al., 2020; Conradt et al., 2023), as infiltration of precipitation water is considered to be the most important groundwater source in Central Europe (Brakkee et al., 2022). ERA5 soil moisture was evaluated for the four soil layers over the period 2018-2020 and compared against the climatology averaged over 1991-2020 in order to assess the strength of the soil moisture deficit and its persistence during the consecutive drought years 2018-2020. For this analysis, time series of daily means as well as centred 92-day running means were computed for all land points of the study area 4°-16° E and 45°-55° N, covering Germany and adjacent regions. The evaluation of soil moisture in the lowest soil layer also gives an indication of the groundwater reservoir as it interacts with the aquifer in the modelling system (Cerlini et al., 2021).

2.5 Agricultural and hydrological drought of the year 2018

Lack of sufficient soil moisture, resulting from shortage of precipitation and excess evapotranspiration leads to agricultural drought. Lack of run-off and surface water result in hydrological drought (streamflow deficits) (Seneviratne et al., 2021). To estimate the severity of agricultural and hydrological droughts across Europe during summer 2018, we employed the nitrogen version of the vegetation, crop, and hydrology model LPJmL (Schaphoff, et al., 2018; von Bloh et al., 2018; Lutz et al., 2019; Herzfeld et al., 2021). The analysis is based on 69 years (1951-2019) obtained from model simulations driven with daily temperature, precipitation, and radiation data from the GSWP-W5E5 dataset (Kim, 2017; Cucchi et al., 2020; Lange et al., 2022) at 0.5 arc-degree resolution. To assess agricultural drought, the evapotranspiration deficit calculated as the ratio of actual evapotranspiration to potential evapotranspiration (ET/PET ratio) over the growing season of maize in each year is determined and a generalised beta distribution (a three-parameter probability distribution for variables in a bounded interval) is fitted to the 69 annual values in each grid cell. An ET/PET ratio of less than 1 indicates water deficit or water stress. For the assessment of the hydrological drought, the average river discharge (Dis) during the summer months (June, July, and August) of each year is determined and a generalized gamma distribution (a three-parameter probability distribution for non-negative variables) is fitted to the 69 annual values in each grid cell. Using the fitted distributions, the return period of the conditions in 2018 is determined. To support comparability with other drought indices such as the Standardized Precipitation Evapotranspiration Index (SPEI), the drought severity is also calculated, which is the probability (inverse of return period) of a given year expressed as its distance from the mean (in number of standard deviations) in a standard normal distribution (McKee et al., 1993; Vincente-Serrano et al., 2010). For example, a return period of 44 years is equivalent to the 2.28th percentile, which is -2 standard deviations away from the mean and would be assigned a drought severity of -2.

2.6 Impact on the agricultural production of 2018

In comparison with the past three decades, the year 2018 was identified as a year with severe winter wheat yield losses estimated using a compilation of LOESS (locally estimated scatterplot smoothing; to take into account improvement of agricultural practises (Zampieri et al., 2017)) detrended and gap-filled yield data at county level aggregated from a variety of sources including the Regionaldatenbank Deutschland (Statistische Ämter des Bundes und der Länder, 2021) and the Statistical Offices of the federal states of Germany (Ellsäßer and Xoplaki 2022abc; Ellsäßer and Xoplaki, 2024). The resulting annual gridded yield data was evaluated using the Standardized Yield Anomaly Index (SYAI) that expresses yield anomalies in terms of standard deviation from a 30-year time series. The analysis is based on the Heat Magnitude Index (HMD) (Zampieri et al., 2017), the drought index SPEI (Vicente-Serrano et al., 2010) and the Combined Stress Index (CSI) (Zampieri et al., 2017) that accounts for stress compounds of heat and drought through a (ride-regression based) superimposition of HMD and SPEI, using the temperature and precipitation series from E-OBS (Cornes et al., 2018). In order to derive crop relevant results, all indices were evaluated for the most vulnerable stages of phenological crop development according to the specific region using the German Weather Service (DWD) phenological data set (Kaspar et al., 2015). A spatially explicit linear regression between

yield anomaly and stress indices was computed for time series covering the past three decades and the coefficient of determination (R^2) was calculated to express the proportion of yield anomaly that can be explained by heat, drought or compound stress.

2.7 Loss and damage of compound vs. non-compound wind extreme events of the winter 2018

The precipitation-wind storyline starts with a description of the synoptic situation during the winter season 2018. The cyclone track analysis in this section is based on the cyclone tracking methodology of Murray and Simmonds (1991) and Pinto et al. (2005) applied to ERA5 data (Hersbach et al., 2020).

Loss and damage in this section is defined according to the UN Framework Convention on Climate Change (UNFCCC) as the harm caused by anthropogenic (human-generated) climate change (UNFCCC, 2021; OECD, 2021 and references therein). For the quantitative assessment of the impact of CEs in terms of loss and damage, a compound wind and precipitation extreme is defined when both variables exceed their local 98th percentile (Martius et al., 2016). For winter events, these percentiles are calculated using data from the December to February season. Co-occurrence is defined when wind gusts and precipitation both exceed their respective 98th percentile at a specific grid box, with precipitation exceedance occurring on the same day, the day before, or the day after, within a 50 km radius around the grid box centre.

The daily loss data for residential buildings accumulated over Germany provided by the German Insurance Association (GDV) are categorised by days on which a CE occurred and days on which it did not. This results in two separate loss distributions for compound and non-compound events.

2.8 Concurrent heavy rain and storm extremes – estimation of probability of event occurrence

The estimation of the probability of occurrence of compound heavy rain and wind is carried out on precipitation and wind time series from DWD weather stations. Multivariate distributions in the form of copulas are used to determine the probability of occurrence of combined events. Copulas make it possible to model the dependency structure of the variables under consideration independently of their marginal distributions (e.g. Manning et al., 2024 and references therein). This allows for the use of any distribution function for the marginal distributions.

We carried out fitting tests for both the marginal distributions and the copulas. However, Archimedean copulas are generally preferred when dealing with hydrological parameters (Bender, 2015; Jane et al., 2020). In this particular case, the Frank copula (Frank, 1979) was chosen as the most appropriate option. The Frank copula is a one-parametric copula in which the copula parameter *theta* can be determined from the correlation between random variables. The approach treats the extremes of the two variables (rain and wind) separately. The annual maximum values (AMAX) are extracted from the time series and tested for statistically significant trends using the Mann-Kendall test at a 5% significance level. Stationary methods of extreme value statistics are applied, requiring the assumption of independence and identical distribution of all time series. Consequently, series with significant trends are homogenised using linear regression. The distribution parameters of the strong wind and precipitation data sets are then determined using maximum likelihood. In addition, the correlation between heavy rain and

storm is calculated using the Kendall rank correlation. For each AMAX wind value, the concurrent precipitation value is selected and vice versa. To ensure the independence of precipitation events, wet episodes are separated by a dry period of at least as long as the accumulation period. Due to this restriction, not all AMAX wind events can be paired with a precipitation episode, even when precipitation is present, e.g., for longer precipitation durations (>1day) and considering a ±2-day window, no AMAX wind and precipitation episode pairs exist. Subsequently, these pairs of values are applied to adjust the marginal distributions and copulas, thereby determining the combined probabilities of occurrence.

2.9 Rockfall events

Rockfall is an impact that can be triggered by extreme precipitation (e.g., Nissen et al., 2022). Favourable preconditions, such as previous freeze-thaw cycles and enhanced sub-surface moisture, increase the susceptibility for such events. A logistic regression model, describing the probability of rockfall in the Central European low mountain ranges as a function of meteorological (pre-) conditions, was fitted using the Rupp and Damm (2020) database of rockfall events. To find the optimal statistical model, a large number of models including different atmospheric predictors and interaction terms between the predictors were compared. The best model was selected based on the logarithmic skill score determined during cross validation. The best-performing model includes across-site percentile of a fissure water proxy D (precipitation minus potential evaporation determined for the last 5 days), the local percentile of daily precipitation and the binary information if a freeze-thaw cycle has occurred within the last 9 days. It also considers the interaction between daily precipitation and D. By including several meteorological parameters the statistical model describes the multivariate compounding nature of rockfall initialization. By taking preconditions into account the preconditioned compounding component is addressed. Using the statistical model, a probability for a rockfall event can be determined for each day from the meteorological conditions of the previous 9 days and the day itself. Details of the statistical model can be found in Nissen et al. (2022).

2.10 Convective cluster events of the summer 2018

Convective cluster events (CCEs) are spatially connected areas of intense lightning activity that occur simultaneously in the same geographic region. CCEs can be detected using the Spatial-Temporal Density-Based Spatial Clustering of Applications with Noise (ST-DBSCAN) algorithm (Ester et al., 1996; Birant and Kut, 2007). The data used are cloud-to-ground lightning strokes from the European Cooperation for Lightning Detection (EUCLID) network (Schultz et. al., 2016). ST-DBSCAN is further developed and specifically adapted for the detection of spatio-temporal clustering of lightning strokes (Augenstein et al., 2023). The algorithm identifies arbitrarily shaped clusters in a set of given points, which in this case are spatio-temporally close lightning strokes. For the identification of CCEs, thresholds from sensitivity studies have been used, i.e., if at least 40 lightning strokes occur within 20 minutes and 50 km, single lightning strikes are marked belonging to a CCE. These thresholds have proven to be an “optimal” balance to distinguish between lightning clusters and noise.

2.11 Occurrence of extreme compound events from recent to near-term future climate conditions

The estimation of the projected changes in the frequency of CEs from recent to near-term future climate conditions is based on the 30-member CMIP6 MPI-GE (Olonscheck et al., 2023). The historical and SSP5-8.5 (Riahi et al., 2017) simulations for the periods 1975-2025 and 2025-2075 are used, representing climate conditions that for the CMIP6 MPI-GE range from about 1 to 3 °C increase in global mean surface temperature since pre-industrial times (Olonscheck et al., 2023). The projections cover Germany and more specifically the region defined by the 4°-16° E and 45°-55° N latitude-longitude domain. The compound heat and drought years are defined by the cumulative precipitation from May to October and the mean daily maximum temperature from June to August, spatially averaged over Germany. Extreme compound hot and dry years exceed the 20-year return levels for both precipitation deficit and maximum temperature individually, defined as the 5th and 95th percentiles, respectively, for the period 1975-2025. The compound precipitation-wind years are defined on the winter (December to February) daily mean precipitation and daily maximum surface wind. The selection of events is based on the exceedance of the 98th percentile for wind and precipitation during the period from 1975 to 2025. For each grid cell, wind and precipitation events are identified when they exceed this threshold on the same day, while for precipitation alone, the exceedance can occur either on the same day or the day after. The cumulative effect for the whole season is the sum of all daily occurrences over all winter days and each grid cell. Extreme compound wind and precipitation years exceed the 20-year return levels for precipitation and wind individually, defined as the 95th percentile of each variable for the period 1975-2025.

2.12 Representation of moisture availability of 2018 in model simulations

The performance of model simulations in realistically representing drought conditions like those of 2018 and the 2018-2020 three-year drought cluster of events is assessed based on the estimated trend of the warm season (March to August) moisture availability in Germany. Drought conditions are described with the SPEI index (Vicente-Serrano et al., 2010) for observations, using ERA5 data (Hersbach et al., 2020) for the period 1979-2019, and for bilinearly interpolated (regular 0.5° lon-lat grid) and extended to 2021 ensemble simulations of CMIP5 (Taylor et al., 2012; Aalbers et al., 2023) global circulation models and of EURO-CORDEX 0.11° (Giorgi et al., 2009) regional multi-model ensemble for the historical (1950-2005) and the near-to-mid-term future (2006-2070) periods under RCP8.5. The linear trend of the 3-year running mean for the March to August intervals is calculated over the periods 1975-2021 for the simulations (1979-2019 for ERA5) and 2022-2070 in order to account for the transition from dimming to brightening regime in the 1970s (Wild, 2009, 2016).

3 Compound events in the year 2018

3.1 Temperature-precipitation compound events during 2018

The exceptionally hot and dry conditions in 2018 extended over larger areas including central and northern Europe and were associated with impacts on various economic sectors (e.g. Toreti et al., 2019a; Zscheischler and Fischer, 2020; Bastos et al., 2023; Conradt et al., 2023; Shyrokaya et al., 2024).

3.1.1 Drivers of the hot summer of 2018

The 2018 heatwave was a spatially CE featuring concurrent heatwaves in Scandinavia and central Europe (Spensberger et al., 2020; Rousi et al., 2023). Prior to the 2018 heatwave, a striped high-pressure system formed over northern Europe in late June, during a combination of the positive phase of the North Atlantic Oscillation and the Rossby Wave 7 pattern (Drouard et al., 2019; Kornhuber et al., 2019). Figure 1 presents the jet stream state during the 2018 summer and the heatwave day frequency for each grid point over the Eurasian sector. During the intense European summer heatwave, a large blocking system at 500 hPa, and a double jet stream configuration is visible in the 250 hPa zonal wind field (Kornhuber et al., 2019; 2020; Rousi et al., 2023, see Methods section 2.1). Heatwave hot spots over Europe coincide with areas of weak winds between the polar and subtropical jets. Such large-scale atmospheric conditions are conducive to the occurrence of extreme events over Europe, in particular to heatwaves near the centre of the blocking system (see Kautz et al., 2022 for a review). In particular, the hot summer of 2003 (western/central Europe, Luterbacher et al., 2004; Fink et al., 2004; Fischer et al., 2007; García-Herrera et al., 2010) and 2010 (heatwave over western Russia, Barriopedro et al., 2011; Di Capua et al., 2021; Rousi et al., 2022) were characterised by similar large-scale conditions.

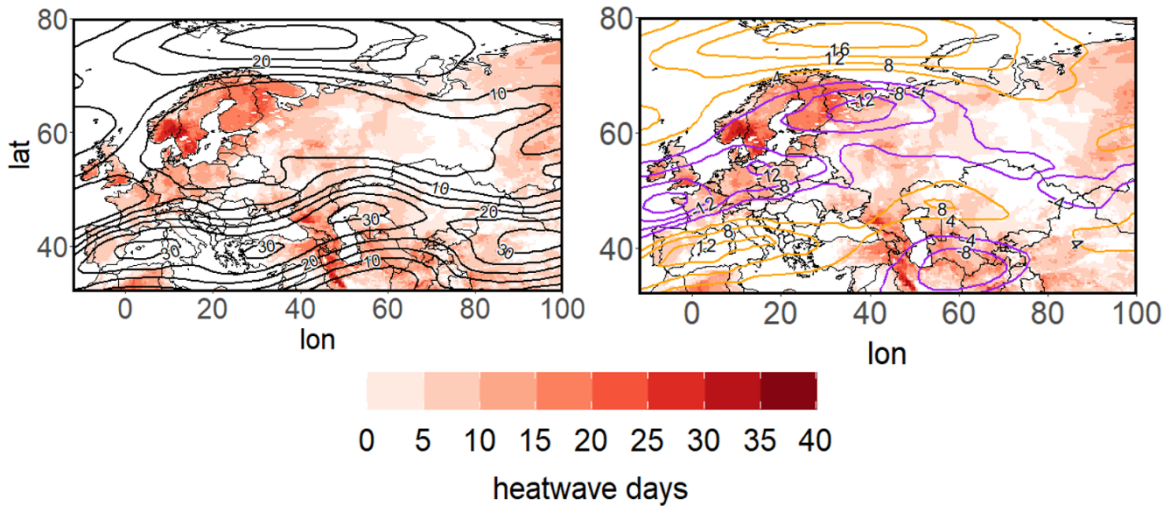

Figure 1: Jet stream state (contour lines) and heatwave days in summer 2018 (shading). Left: zonal wind at 250 hPa (black contours from 5 m/s to 30 m/s every 5 m/s); Right: zonal wind anomalies at 250 hPa (anomalies based on 1979-2020 July climatology and plotted with contours from -16 m/s to 16 m/s every 4 m/s, negative anomalies are shown in purple contours and positive in orange) for the period 4-25 July 2018, the longest period of consecutive double jet states. All fields stem from ERA5 reanalysis data (Hersbach et al., 2020).

3.1.2 Detection of spatial patterns of extreme events

During the summer 2018, large-scale temperature (T2m) and precipitation deficit (PD) patterns characterize the exceptional conditions. Figure 2 shows the analysis of typical pattern of common extremes and their expression during the 2018 heatwaves at the European scale based on cross-TPDM and EPI (see Methods section 2.2). In July-August 2018 the pronounced heatwave is accompanied by extreme EPI^{PD} preceding the heatwave for several days. This heatwave is considered the most prominent event in the period under consideration (see also Liu et al., 2020). The negative eigenvector anomalies of the second mode (Fig. 2a,b bottom left) mostly cover the regions identified as heatwave spots in Figure 1. Thus, the anomalies in the second mode expansion coefficients (Fig. 2a,b bottom right) indicate the beginning of the heatwave, which initially affected northern Europe (i.e., Finland, Norway, and northwestern Russia). From mid of June onwards, there were extremes in PD, particularly in Central Europe, as indicated by the third mode of the expansion coefficient (Fig. 2c,d bottom right). By the end of July 2018, the heatwave extended to Central Europe as evidenced from the abrupt change of sign in the third mode expansion coefficient (Fig. 2c,d bottom right).

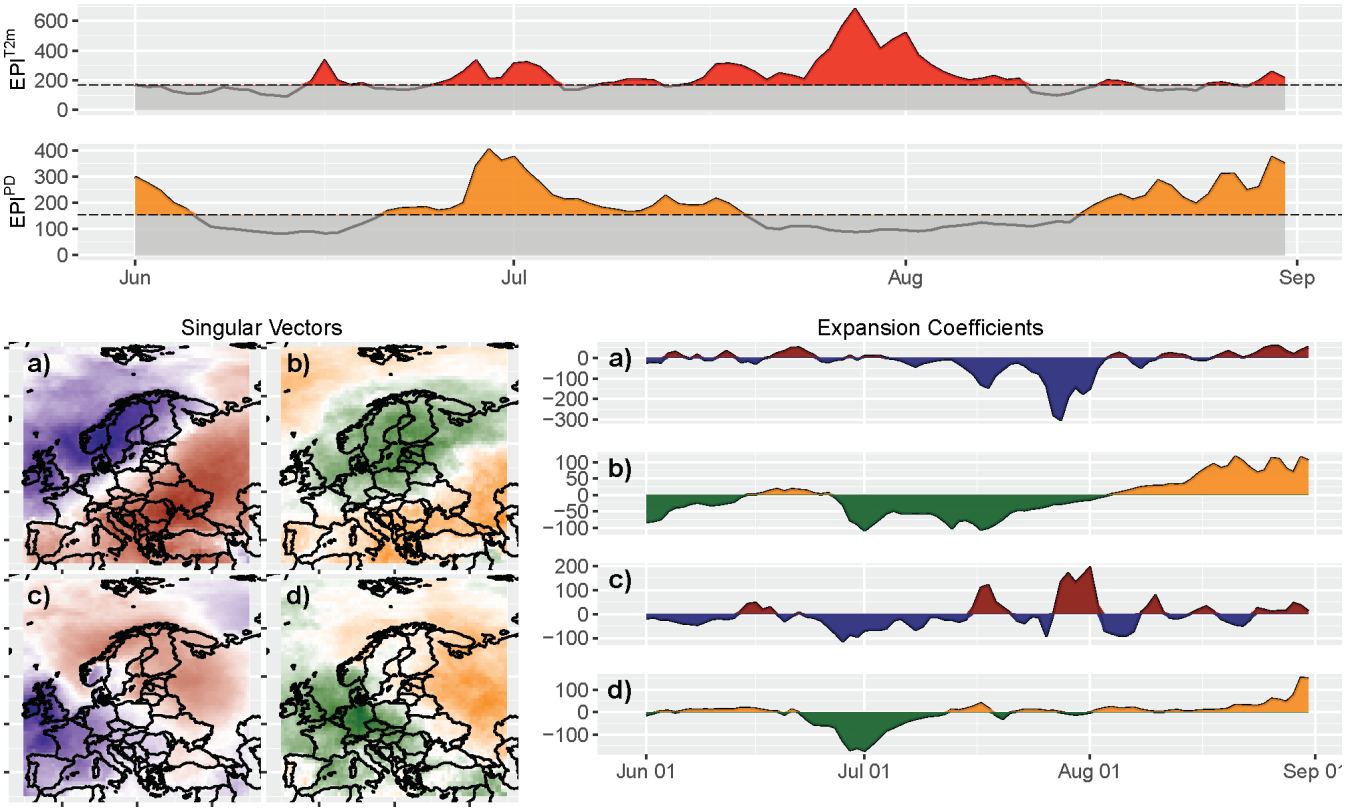

Figure 2: Top: Extreme Pattern Index (EPI) for T2m surface temperature (EPI^{T2m}, red) and precipitation deficit (EPI^{PD}, orange) for northern Hemisphere 2018 summer months. Values exceeding the 80th percentile are considered to identify extreme events in PD and T2m from EPI and are highlighted in red/orange, respectively; Bottom left: second (a, b) and third (c, d) singular vectors (CVs) associated with large-scale temperature (blue/red) and precipitation deficit (green/orange) pattern; Bottom right: second (a,

b) and third (c, d) expansion coefficient for northern hemisphere 2018 summer months. Positive values are plotted in red/orange and negative values in blue/green.

3.1.3 Surface water storage of the dry summer of 2018

The high temperature in 2018 was mainly due to increases in the amount of net surface radiation caused by the clear skies associated with reduced precipitation (Liu et al., 2020). Germany experienced a strong increase of net radiation of approximately +31%. Liu et al. (2020) report that land cover played a critical role in determining the occurrence and strength of soil moisture-temperature coupling, i.e. cropland/grassland depletes soil moisture more readily than forests, thereby triggering a more rapid release of sensible fluxes a major feature observed during the 2018 heatwave. During the 2018 heatwave, because of different soil moisture conditions, latent flux in Germany decreased by 12% and sensible flux significantly increased by 122% (Liu et al. 2020). Further, Bastos et al. (2020) used 11 vegetation models and showed that spring conditions promoted increased vegetation growth, which, in turn, contributed to fast soil moisture depletion, amplifying the summer drought. Figure 3 presents the groundwater memory in the summer 2019 of the ensuing hydrological year 2018/2019 for each of the 20 European river basins on the following year's summer surface water storage (S_u).The ensemble simulations indicate that following the 2018 drought the conditional probability that the autumn of the hydrological year 2018/2019 (August to November 2018) is anomalously dry $p(S_{u,d})$ is 95.5% with a 100 ± 0.0% confidence with respect to the climatological variability. In the following seasons, $p(S_{u,d})$ and the associated confidence decrease due to the increasing influence of the uncertainty in the atmospheric conditions. Specifically, for winter $p(S_{u,d})$ is 81.8% with a confidence of 99.5 ± 0.3%, for spring (March to May 2019) 63.6% with a confidence of 80.2 ± 6.0% and for summer (June to August 2019) of the hydrological year 2019/2020 $p(S_{u,d})$ is 68.2% with a confidence of 90.1 ± 3.7% with respect to the climatological variability. Without considering the groundwater storage memory effect, a probability of a dry surface water anomaly $p(S_{u,d})$ of ~ 50% would be expected due to the atmospheric uncertainty accounted for in the ensemble of realisations at the interannual time scale. Taking drought as a precondition for S_u on this scale, the analysis shows that even one year later a $p(S_{u,d})$ of 68% is still well above 50% at a confidence level of 90 ± 4%. Thus, statistically, groundwater storage takes longer than a year to fully recover from a drought influencing surface water storage, independent of the ambient atmospheric conditions (Lorenz et al., 2010; Orth and Seneviratne, 2012; Song et al., 2019). Recent evidence points to the fact that the impact of global warming on soil moisture drought severity in west-central Europe such as the case in 2018 is increased. The drought risk is strongly enhanced by the drought intensification and increase in frequency, yielding shorter recovery time between events for nature and society (Aalbers et al., 2023).

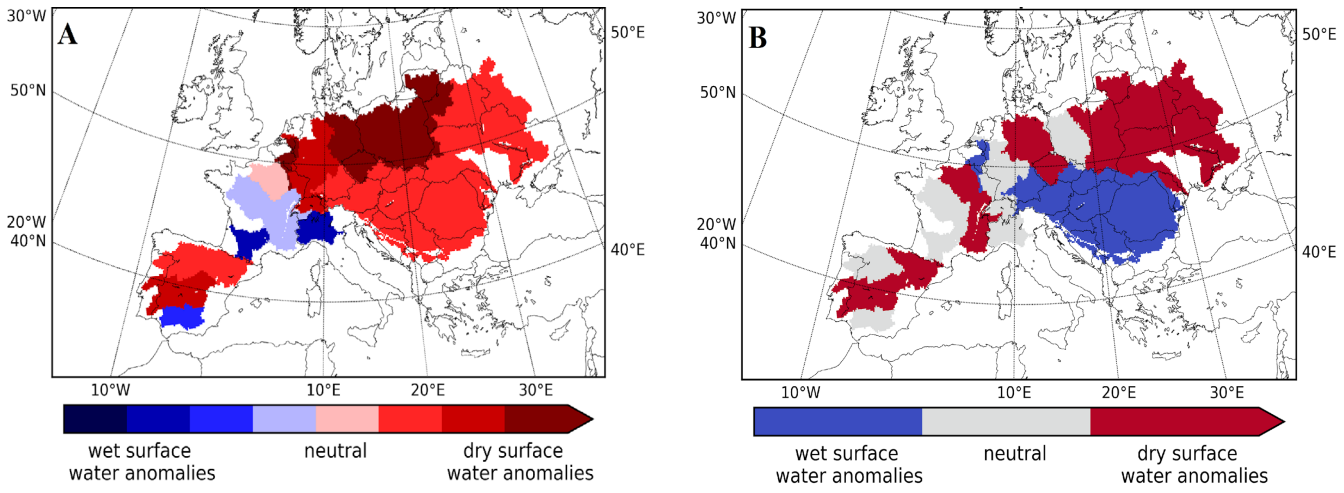

Figure 3: Averaged impact of the yearlong 2018 drought on the following year's summer (June to August 2019) surface water storage (S_u) anomaly per river basin (see Methods section 2.3). A: S_u anomaly in 2018 for each river basin in quartiles; B: S_u anomaly in the summer (June to August 2019) after 2018 initial conditions and (ensemble) mean of 22 atmospheric conditions.

3.1.4 Soil moisture of the dry summer of 2018

To address sectoral impacts (e.g. Conradt et al., 2023), we focus on the effects of the 2018 drought on agriculture and forestry in Germany. For this purpose, the temporal evolution of soil moisture deficits at different depths from the ERA5 dataset and agricultural data from German national institutes such as the Statistisches Bundesamt (Destatis) are analysed. Focusing on the temporal evolution of soil moisture, a deficit developed during the spring and early summer of 2018 (Rousi et al., 2023), which also reached the lowest soil layer with a temporal delay of about three months, as shown in Fig. 4. The dryness in 2018 was more intense than the usual soil moisture variability in the period 1991-2020, as shown by the soil moisture dropping below the range of ±1 standard deviation of the 1991-2020 mean soil moisture (shaded area). While the moisture in the three upper soil layers mostly recovered during the following winter 2018/2019, the moisture did not percolate down to the lowest soil layer, which remained in a dry anomaly. The recurrent drying of the upper layers in spring and summer 2019 inhibited considerable infiltration, so that the moisture deficit of the lower soil layer persisted until winter 2019/20, when the relatively wet climatic conditions allowed a recharge of the lower soil layer moisture reservoir (Brakkee et al., 2022) and thus probably also of the groundwater (e.g., Brauns et al., 2020). Hence, the lack of soil moisture reached the entire soil column and thus the entire root zone of the vegetation during the summers of 2018 and 2019, placing the vegetation under soil moisture stress (Tijdeman and Menzel, 2021).

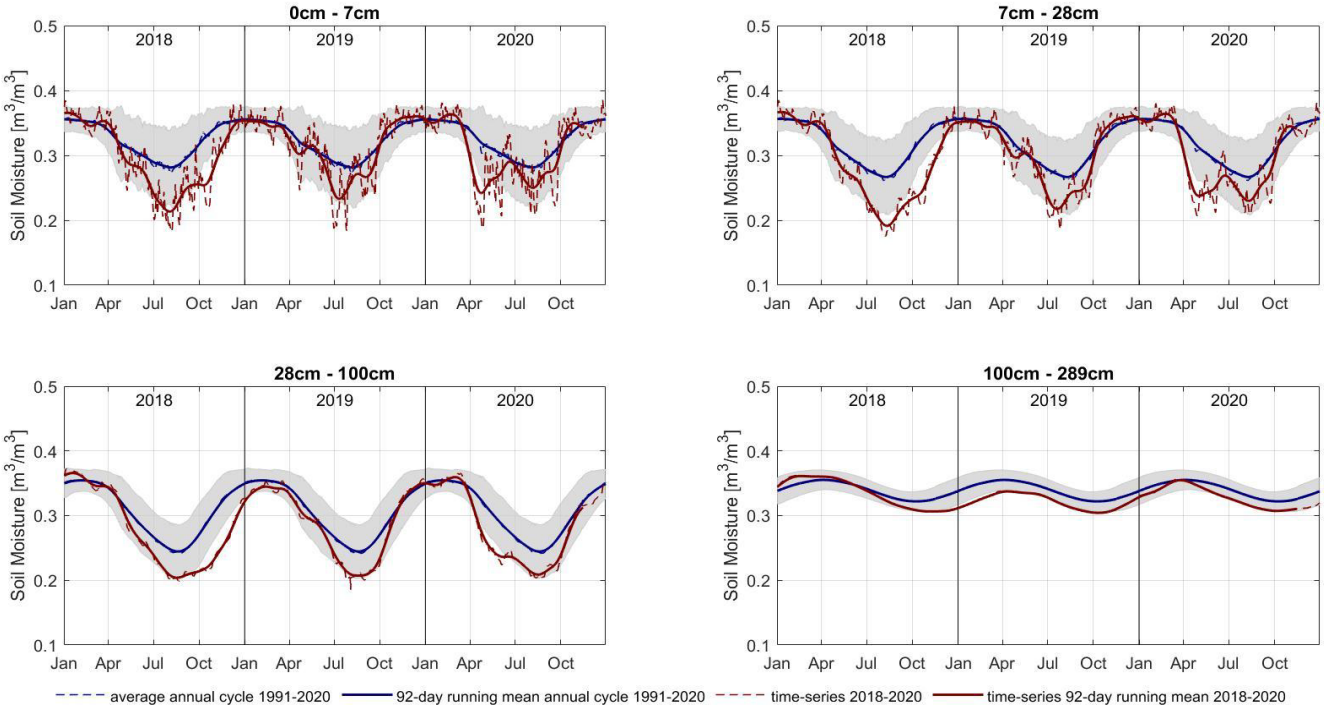

Figure 4: ERA5 soil moisture in four different layers from surface (0 - 7 cm) to a depth of 2.89 m (100 - 289 cm) with two intermediate layers 7 - 28 cm and 28 - 100 cm depth. The red dashed line denotes the daily mean and the solid red line denotes the 92-day running mean in 2018-2020. The annual cycle of soil moisture with a daily resolution (dashed blue line) and the average running mean (solid blueline) are also shown. The grey shading indicates a range of ±1 standard deviation of soil moisture over the period 1991-2020 indicating the normal year-to-year variability of the soil moisture.

3.1.5 Agricultural and hydrological drought of the year 2018

The anomalous soil moisture conditions are reflected in an anomalous low ET/PET ratio over the summer months (June, July, August), indicating a severe agricultural drought (Fig. 5, left). In almost the entire northern part of Germany, the agricultural drought index exceeds -2.5, which is equivalent to a return period of more than 160 years, an estimate associated with uncertainties. However, the agricultural drought is not limited to northern Germany but comprises large parts of central, northern, and northeastern Europe. The low soil moisture conditions also lead to a hydrological drought (low river flow) over the summer months (Fig. 5, right). However, the severity and spatial pattern of hydrological drought differs from the pattern of agricultural drought because propagation from soil moisture drought to hydrological drought takes time and typically leads to a lagged occurrence (Van Loon and Van Lanen, 2012) and a longer persistence (see section 3.1.3 on Surface water storage). Another reason is that hydrological drought can spread along the river network affecting regions unaffected by low soil moisture (e.g., along the Danube river in eastern Europe). Nevertheless, in many parts of Germany and northern Europe, agricultural and hydrological drought coincided in the summer of 2018 (Blauhut et al., 2022), affecting the possibility to

irrigate as a means to alleviate the agricultural drought. This provides an example of how co-occurring impacts (droughts) can amplify each other to cause even greater secondary impacts (agricultural yields, see section 3.1.6 on Impact on the agricultural production) in a similar way as co-occurring meteorological conditions trigger CEs.

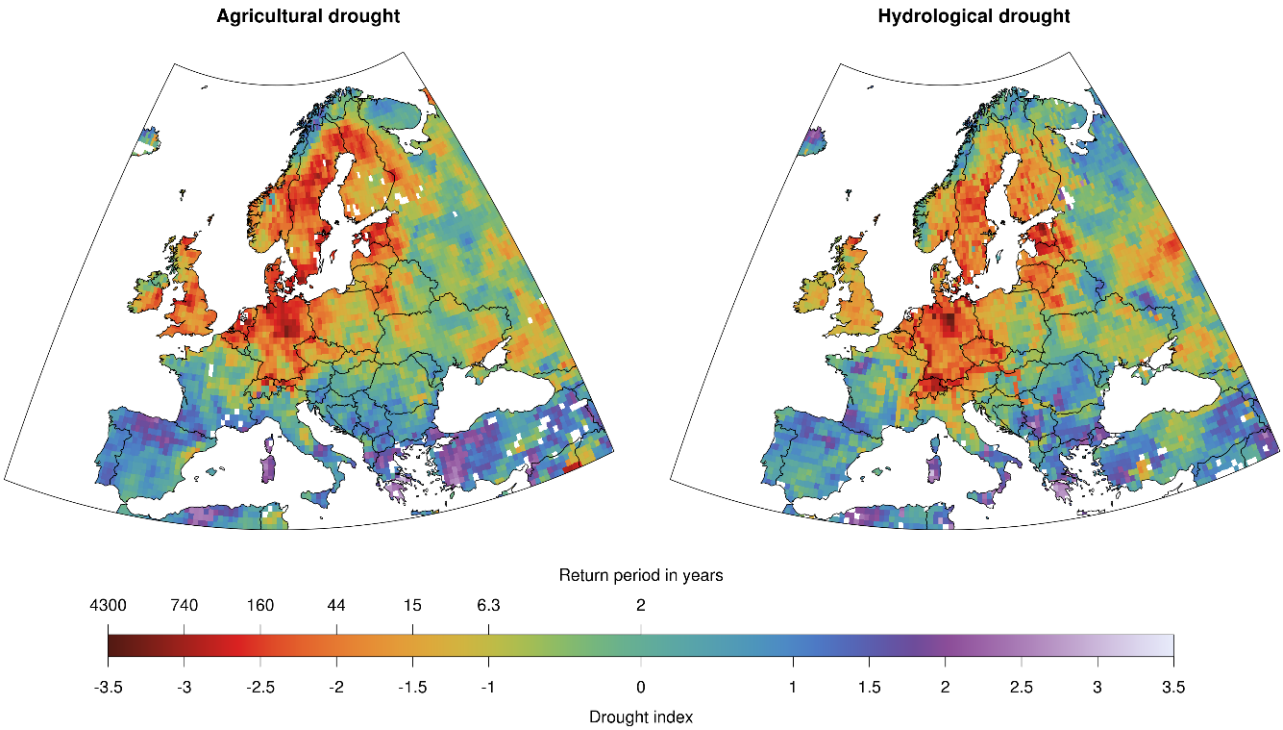

Figure 5: Drought severity and return period of agricultural and hydrological drought during summer 2018. Note that drought severity (as expressed by the drought index) and return period are closely related (see Methods section 2.5).

3.1.6 Impact on the agricultural production of 2018

In Germany, the hot and dry spring and summer of 2018 had an unprecedented impact on crop yields. Extremely low crop yields (Toreti et al., 2019a; Bellouin et al., 2020; Conradt et al., 2023 for northeastern Germany) led to large insurance claims over agricultural losses and financial support requests by farmers from governments in Germany (EUR 340 million), Sweden (EUR 116 million) and Poland (EUR 116 million) (D'Agostino, 2018; Munich Re 2019). Winter wheat yields were more than 10% below the 30-year average and 13% below the previous three years. In some counties, yields were more than 40% lower than in previous years. Regionally, winter wheat was particularly hard hit in eastern and northeastern Germany, with an average loss of 22% compared to the last three decades. The HMD index and the SPEI indicate a severe heatwave and drought respectively, which was most pronounced in central and northeastern Germany. Figure 6 shows the explained variance of yield anomalies and the stress indices HMD, SPEI and CSI (see Methods section 2.6) revealing a strong connection between these

components. However, not all regions experienced such severe yield losses; winter wheat yield in southwest Germany was hardly affected, with losses of only 1.2% compared to the last three-decade average. A hydrological see-saw with rather wet conditions in southern Europe and the resulting yield increases characterise the unique combination of climatic anomalies in Europe in 2018 (Toreti et al., 2019a). Winter wheat productivity was even positively affected in some regions.

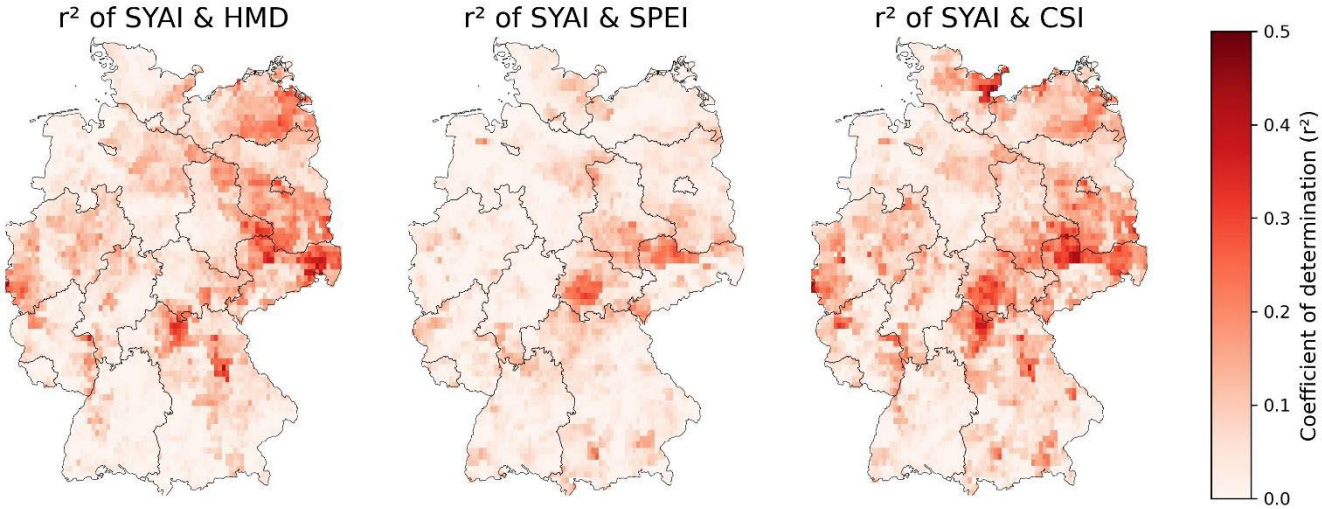

Figure 6: Coefficient of determination of Standardized Yield Anomaly Index (SYAI) and stress indices Heat Magnitude Day (HMD), Standardized Precipitation Evapotranspiration Index (SPEI) and Combined Stress Index (CSI) demonstrate the impact of heat, drought and compound stress over the last three decades on winter wheat in Germany.

3.1.7 Impact on the forests in 2018

The drought of 2018 was likely the largest source for severe forest disturbance in Europe for more than 170 years (Senf and Seidl, 2021), especially in central and northern Europe (Buras et al., 2020). Consequently, in the summer of 2018, about 11% of the central European forest area experienced early wilting (Brun et al., 2020), resulting in a large reduction in greenness (Schuldt et al., 2020; the three aforementioned studies are based on NDVI data). The 2018 drought continued into 2019, making the consecutive European droughts of 2018 and 2019 unprecedented in the last 250 years (Hari et al., 2020). The low soil moisture content in 2018 and an increased water-vapour pressure deficit in the following two years were the main drivers for the forest disturbances of about 4.74 × 106 ha in Central Europe (Senf and Seidl, 2021). The likely cause for these forest damages was that trees under drought and heat stress experience carbon starvation (Bastos et al., 2020) and have risk for embolism, which causes failures in water transport (Allen et al., 2015; Schuldt et al., 2016). The drought and heatwave in that period facilitated outbreaks of bark beetle, enhancing the damage levels to forests. As such, insect outbreaks in Central Europe had a 2-3-fold increase in annual losses between 2017 and 2018 (Hlásny et al., 2019) and extraordinary mortality and damage occurred during 2018 in Sweden due to rapid beetle population growth (Öhrn et al., 2021). Although wildfires have decreased

on a global scale recently, Central Europe is likely to face larger and more frequent forest fires (Feurdean et al. 2020, Milanovic et al. 2020; Carnicer et al., 2022), which can have severe environmental, economic and social consequences (Lidskog et al. 2019).

3.2 Precipitation-wind compound events during 2018

In this section, CEs that involve heavy precipitation and strong winds are described. Examples include two January windstorms (Friederike and Burglind) and several weeks of convective activity in May and June of 2018.

3.2.1 Loss and damage of compound vs. non-compound wind extreme events of the winter 2018

On January 16, windstorm Friederike formed as a low-pressure system near Newfoundland. Within the next two days, Friederike intensified and quickly travelled across the Atlantic (Fig. 7), losing its closed structure at 1800 UTC on 17 January. Friederike re-intensified over the British Isles on 18 January while crossing the jet streak towards the northern jet exit region, a behaviour favourable for intense windstorm development (e.g., Pinto et al., 2009). The storm moved eastward over the North Sea, Germany and Poland, and weakened after 19 January over eastern Europe (Fig. 7a). Analysing the compound character of Friederike around peak intensity using the hourly ERA5 reanalysis data (Fig. 7b,c), the typical near-surface wind and precipitation structure of intense extratropical cyclones is found (e.g., Dacre et al., 2012). Strong 10 m wind gusts (maximum values of 34 m/s relative to the Earth's surface) were present behind and to the right of the eastward moving cyclone centre. Heavy precipitation occurred at both the warm front to the northeast of the centre, wrapping around as the cyclone approached its mature stage, and along the east-southwest stretching cold front (Fig. S1a). During the 12 h period when Friederike passed through Germany from 0600 UTC to 1800 UTC on 18 January, the persistently active warm front left a widespread footprint near the northern edge of the cyclone centre (Fig. 7b) with ERA5 accumulated precipitation exceeding 17 mm. Meanwhile, the cold front contributed to a high precipitation rate (> 4 mm/h based on ERA5) along a narrow west-east oriented band across northern France and southern Germany (Fig. 7c). The co-occurrence of strong winds and heavy snowfall gave to this storm the risk and damage characteristics of a CE (Fig. 7b,c). The highest damages were reported in Ireland, Great Britain, northern France, Belgium, the Netherlands, Germany, Czech Republic and Poland, where gust measurements suggested wind speeds of the order of 100 – 150 km/h. At higher altitudes the observed wind gusts reached 173 km/h at the Sněžka in Czech Republic and 203 km/h at Brocken in Germany (Haeseler et al., 2018). Wind and snowfall associated with Friederike caused further traffic disruption, power outages, property damage including falling trees, and several deaths. Friederike was the strongest storm affecting central Germany since windstorm Kyrill in 2007.

Another CE affecting Germany in the same month was the windstorm Burglind, which formed on the 2nd January 2018. The depression intensified rapidly as it moved eastwards towards the British Isles (Fig. 7a). It reached a peak intensity of 968.9 hPa at 0600 UTC on 3 January 2018 over the North Sea, followed by a weakening over the Baltic Sea. The long active cold front affected a large area of western Europe (Fig. S1b). Heavy precipitation with daily values > 30mm led to rapid snowmelt and massive flooding in many regions. Around the time of the peak cyclone intensity, widespread areas were simultaneously

affected by high precipitation intensities (> 4 mm/h) and high wind gust (~100km/h) (Fig. S1c,d). Further detailed information on Burglind can be found in Eisenstein et al. (2022, see their section 5). Compared to storm Friederike, the compound features of Burgling were more strongly shaped by orography.

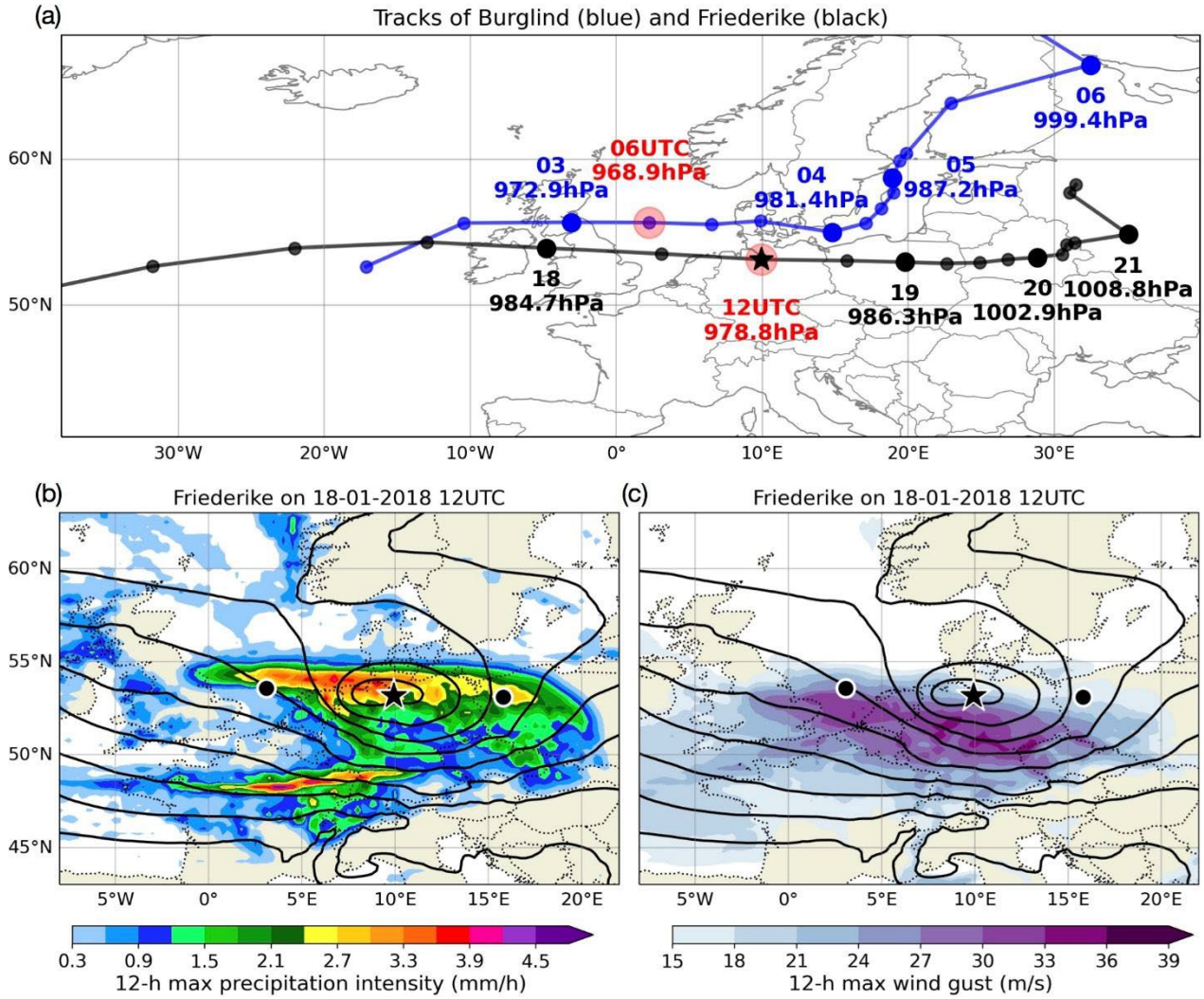

Figure 7: (a) Cyclone tracks of windstorms Friederike (black) and Burglind (blue) in January 2018. Big circles show locations at 0000 UTC on the day as indicated, with the central pressure noted below. Red circles indicate their lifetime peak intensity based on the minimum pressure. (b) Mean sea level pressure (thick contours; increasing from 960 hPa with 5 hPa intervals) at 1200 UTC on 18 January 2018 (location of Friederike shown by the star) and maximum precipitation intensity (shaded) during the period 6 h before and after (locations shown by black circles). (c) Same as b, but for the wind gust at 10 m height (shaded). All fields are derived from the ERA5 reanalysis (Hersbach et al., 2018).

Although the co-occurrence of extreme wind and precipitation is discussed in previous studies for specific events (e.g. Fink et al., 2009 for storm Kyrill) or globally (Martius et al., 2016; Messmer and Simmonds, 2021), there are no studies so far quantitatively evaluating the effect in terms of loss damage. To distinguish between single extreme wind speed events and compound extreme wind speed and precipitation events, we follow the definition of Martius et al. (2016), where both variables are considered simultaneously (see the Methods section 2.7). The loss damage distribution for compound and non-compound events determined from loss data of the GDV is depicted in Fig. 8. For Friederike, there are three days where a co-occurrence of wind and precipitation extremes can be identified over Germany, i.e. 17, 18, and 19 January 2018. The loss ratio for these three days is marked with blue dots in the right column of Fig. 8. The GDV Naturgefahrenreport (2019) reports 900 Million € loss damage for Germany with respect to Friederike. To this date, it was the most damaging winter storm of the last ten years.

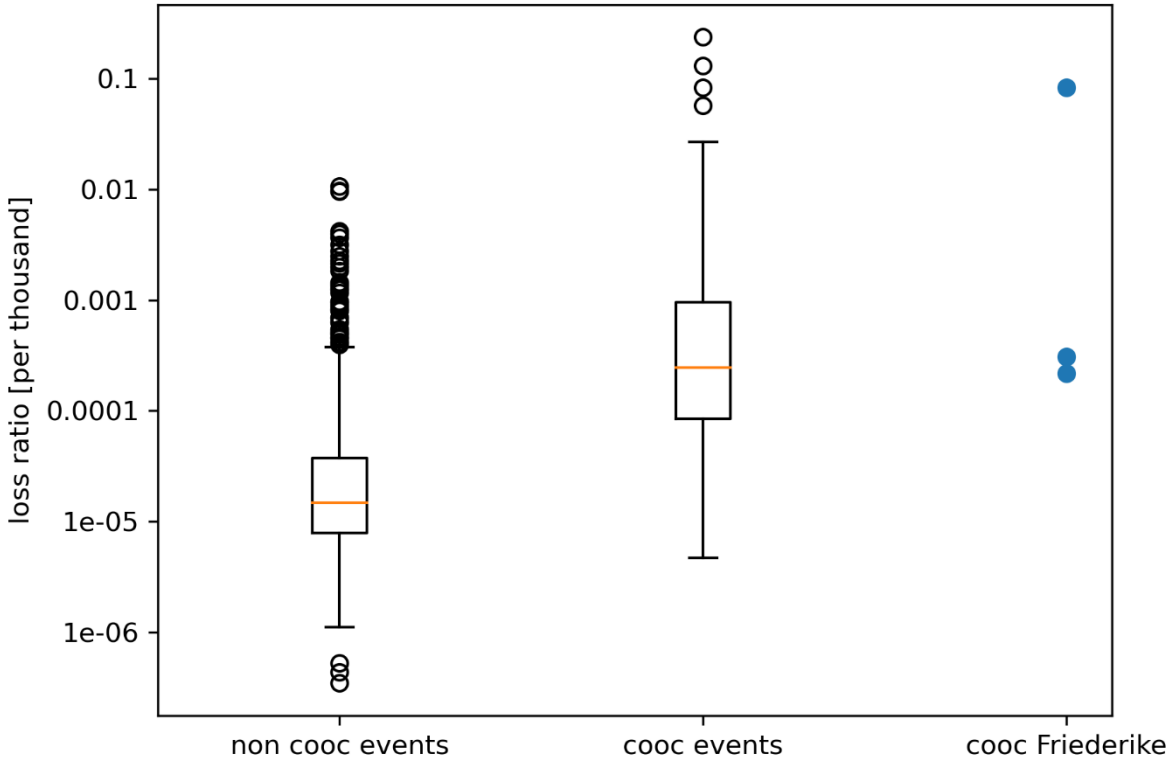

Figure 8: Loss ratio of residential buildings [per thousand] accumulated over Germany for winter events from 1997-2016. Each dot represents one day. Left (non cooc events) bar shows all days which cannot be linked to co-occurrence (cooc) of both extreme wind and precipitation, i.e. single extreme events. Middle bar (cooc events) shows all days which can be linked to co-occurrence of extreme wind and precipitation. Right bar shows the three days for the co-occurrence during windstorm Friederike. The loss ratio is defined by loss normalized with the local sum of insured values.

3.2.2 Concurrent heavy rain and storm extremes – estimation of probability of event occurrence

In a detailed analysis of the probability of co-occurrence of extremes, based on copulas (see Methods section 2.8), the annual maximum values of hourly precipitation and wind speed data at the station Münster/Osnabrück Airport of DWD that are available since 1996 were analysed. The records show an increase in the intensity and frequency of the variables but lack a statistically significant trend. The occurrence probabilities for concurrent precipitation and wind extreme events are shown by the black isolines in Fig. 9. The grey dots are pseudo-observations (artificial precipitation and wind combinations generated using the copula function), while the black, red and green dots mark the observed CEs at the station for each year and the green dot represents Friederike. The distribution of the dots illustrates that - depending on the precipitation duration – wind or precipitation, individually, may not be extreme. A counterexample is the year 2020 windstorm Sabine (red dot; internationally known as Ciara) for which the simultaneous wind and hourly precipitation values both correspond to the respective annual maximum event of that year. The location of the dots relative to the isolines define the return period of the event, where the return period of windstorm Friederike at the station Münster/Osnabrück exceeded 5 years and the one of windstorm Sabine 100 years.

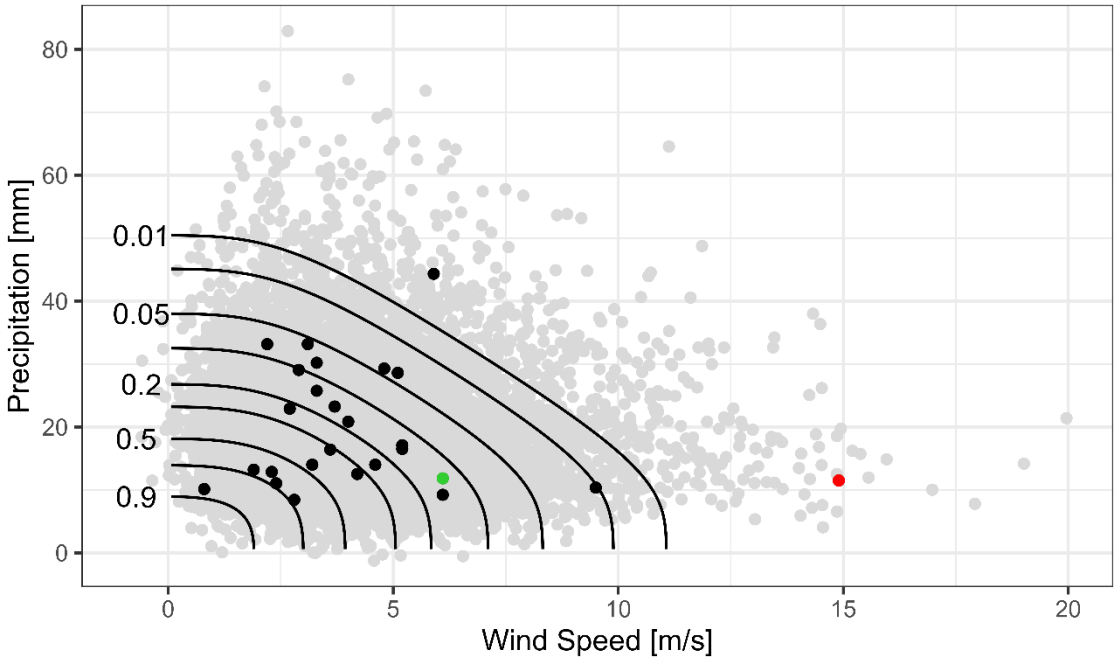

Figure 9: Multivariate analyses for the temporal compound event heavy precipitation and strong wind determined with Copula functions: quantile isolines (lines of equal probabilities), observed event combinations (black dots) and the pseudo-observations (grey dots). Green dot represents storm Friederike (2018) and red dot storm Sabine (2020).

3.2.3 Rockfall events

Another hazard with CE triggers observed in connection with Friederike was a rockfall event. Although wind is normally not considered as one of the triggering factors (D'Amato et al., 2016), such events may also occur as the consequence of the precipitation associated with the windstorm. It is well known that heavy precipitation can initiate landslides and rockfall events (e.g. Nissen et. al., 2022). Slope susceptibility is influenced by pore water/fissure water preconditions, rendering them events with multivariate and temporally compounding triggers. With respect to rockfall, another potentially triggering factor are freeze-thaw cycles prior to the event. In terms of reported hill slope failures, storm Burglind was more effective than storm Friederike. For storm Friederike, only one rockfall event is registered in the landslide database for Germany. The event occurred near Göttingen in Lower Saxony. Figure 10 shows the relationship between the predictors (across-site percentile of a fissure water proxy D -precipitation minus potential evaporation determined for the last 5 days-, the local percentile of daily precipitation and the binary information if a freeze-thaw cycle occurred within the last 9 days) and the rockfall probability expressed as percentage change with respect to the climatological probability. The red dot indicates the conditions on the 18th January 2018 in the area of the event associated with Friederike. The soil at the location was still wet after storm Burglind at the beginning of month and the fissure water (proxy D) at its 83rd percentile. The daily precipitation on the day of the event was 4.5 mm (REGNIE data, Rauthe et al., 2013), which corresponds to the 77th percentile for the given location, assuming immediate melting of the reported snow due to the above freezing air temperature at the event location. The probability of a rockfall event was further increased by pre-event thawing conditions. The logistic regression model suggests that the probability of rockfall on that day was increased by almost 250% (3.5 times more likely) compared to the long-term climatology.

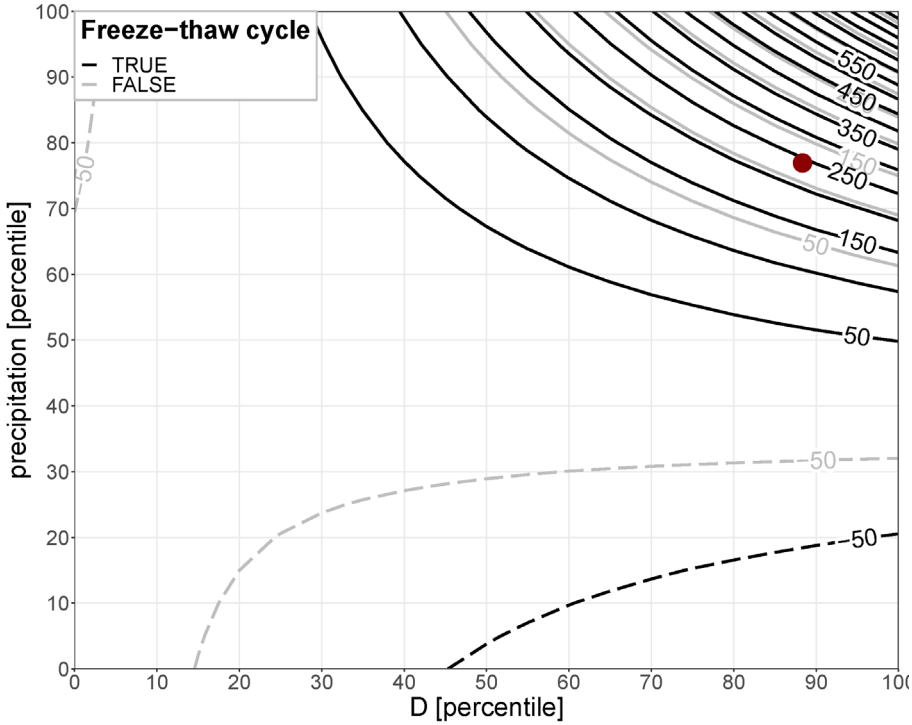

Figure 10: Rockfall probability expressed as percentage change with respect to the climatological probability (isolines) as a function of moisture preconditions (D), daily precipitation and preceding freeze-thaw cycles. The red dot marks the conditions in the vicinity of Göttingen (Lower Saxony) on 18th January 2018.

3.2.4 Convective cluster events of the summer 2018

The spatially as well as temporally compounding nature of severe convective storms (SCSs) can be demonstrated on the example of a three-week series of SCSs in western and central Europe from 22 May to 12 June 2018 leading to the unusual high temporal accumulation of CCEs lasting several days (Fig. 11). During this period, an exceptional persistence of reduced stability combined with sufficient moist air masses caused high thunderstorm activity daily in France, Belgium, Netherlands, Luxembourg, Germany, Switzerland, and/or Austria, associated with precipitation accumulations of up to 80 mm/h within 1 hour and several flash floods (Mohr et al., 2020). The temporal compounding nature of the serial clustering of SCSs over several days to weeks over the same geographic region may increase the probability of flooding and damage. Figure 11b shows a large amount of identified CCEs, especially those with large spatial extent (> 5000 km2), during a three-week period over western and central Europe indicating high thunderstorm activity whose accumulation was unusual (Piper et al., 2016; Mohr et al., 2020). The repeating occurrence is caused by persistent synoptic conditions that favour thunderstorm development over several days to weeks. The presence of atmospheric blocking has been found to be highly conducive to such prolonged thunderstorm episodes, which typically occur on its western and /or eastern flanks (Piper et al., 2016; Mohr et al., 2020; Kautz et al., 2022). Based on statistical analyses, Mohr et al. (2019) found that a block over Scandinavia or over the Baltic Sea

favoured the occurrence of thunderstorms in western and central Europe along the western flank of the blocking system due to of southwesterly advection of warm, moist, and unstable air masses. It is expected that low-frequency modes of climate variability like North Atlantic Oscillation (NAO) or East Atlantic Pattern (EA) could also have an impact on clustered thunderstorm activity over several days (Piper et al., 2019), as these patterns are connected with atmospheric blocking.

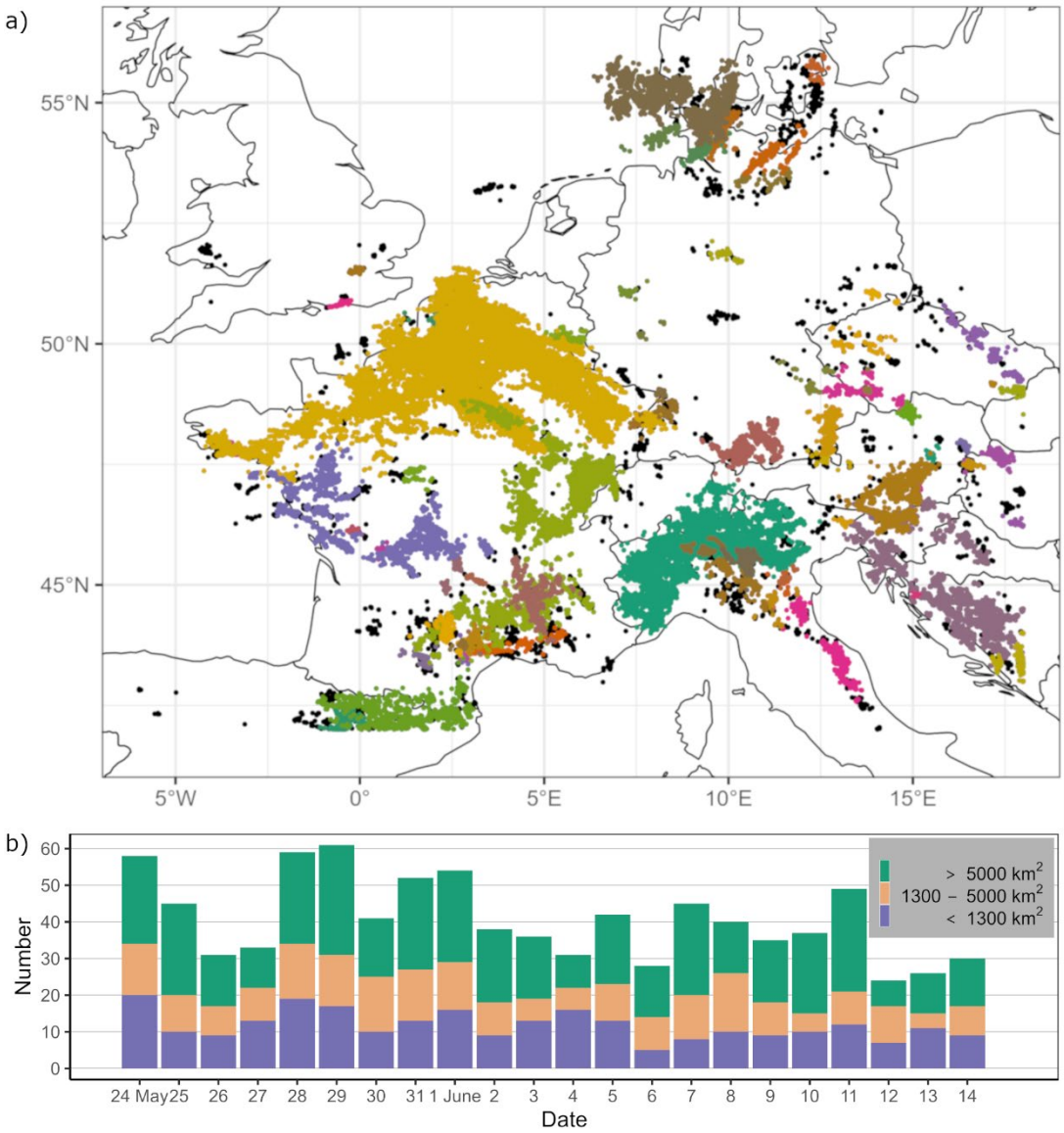

Figure 11: (a) Lightning strokes on the 28 May 2018 in western and central Germany. Each colour represents a convective cluster event (CCE) resulting from the ST-DBSCAN method (see Methods section); black dots represent lightning strokes identified as noise. (b) Daily number of CCEs between the thunderstorm episode from 22 May to 12 June 2018. The colours represent CCEs of different sizes. Note: clusters that overlap are separated in time.

4 Compound events under climate change

In this paper, we have analysed in detail several extreme events that have affected Europe within the calendar year of 2018, starting with the windstorm series in January, followed by a period of heavy thunderstorms in May/June and extended heatwave in July and August which affected various parts of Europe, and the associated drought effects extended well into the autumn season. Our analysis clearly revealed the multivariate and complex characteristics of the events, and thus they can undoubtedly be classified as CEs. The analysis of compound variables was used as a tool to investigate the impacts of man-made climate change. For the two overarching compound types collected in this contribution (hot and dry; wet and windy) we now analyse possible changes of their frequency of occurrence under future climate conditions. Recent studies have provided evidence that regionally extreme hot and dry conditions such as the summer 2018 are expected to become more frequent in the future (e.g., Toreti et al. 2019a; Zscheischler and Fischer, 2020; Aalbers et al., 2023; van der Wiel et al., 2021; Bevacqua et al., 2023). Figure 12 shows a comparison of the occurrence of CEs under recent (1975-2025) climate conditions, with a global mean surface temperature of 1 °C above pre-industrial levels, and under future (2025-2075) conditions of 3 °C above pre-industrial levels, based on the 30-member CMIP6 MPI-GE under SSP5-8.5 (see Methods section 2.11). For drought and heat events, our analysis reveals a clear increase in both the frequency and intensity of extreme compound heat and drought years (Fig. 12, left). Over the past 50 years, extreme compound heat-drought events have occurred with a probability of 1.5%, or about 1-2 times per century. Over the next 50 years, such extreme CEs are projected to become almost 10 times more frequent, occurring more than once every 10 years, and reaching much higher temperatures and precipitation deficits.

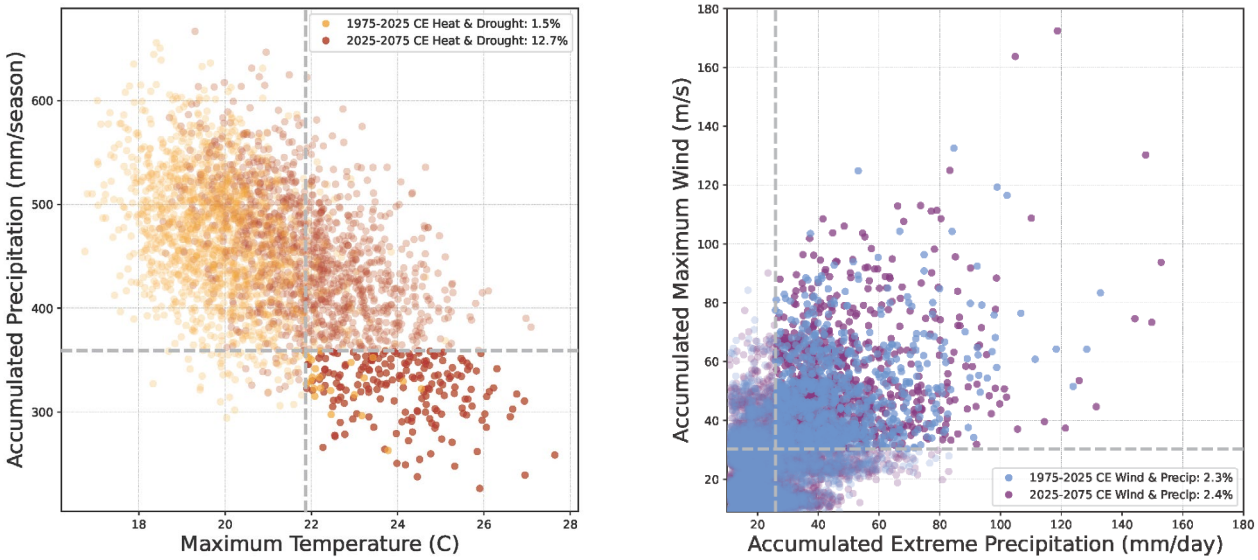

Figure 12: Changes of temperature-precipitation (heat-drought, left) and precipitation-wind (wet-windy, right) compound years occurrence in terms of frequency and intensity, at 1 °C (1975-2025) and 3 °C (2025-2075) above the pre-industrial levels based on the 30-member CMIP6 MPI-GE under SSP5-8.5 (Olonscheck et al., 2023) over Germany.

The likelihood of winters with extreme compound precipitation-strong wind events does not change significantly with global warming in the CMIP6 MPI-GE projections (Fig. 12, right). Such wet and windy winters, where both precipitation and wind are extreme, are projected to occur about once every 50 years. However, although the number of projected events remains roughly the same, the intensity of the actual wind and precipitation levels reached during the most extreme compound wet-windy events increases substantially in the near future. .

A factor that strongly modulates the occurrence of extremes in Europe is the soil moisture availability, as decreasing soil moisture availability initiates a suite of processes feeding back into an intensification of both heat waves and droughts (Miralles et al., 2019). Figure 13 presents a comparison between the observed (ERA5), simulated (extended historical) and projected (RCP8.5) drought conditions via the SPEI moisture availability index (see Methods section 2.12). For the historical period 1979-2019, the reanalysis shows trends in the 3-year running mean SPEI, with a clear drying tendency in central and southern Germany during the warm season, with lower values elsewhere in Germany (Fig. 13a). Part of this trend may be related to the multi-year drought of 2018-2020 at the end of the time series. The CMIP5 multi-model ensemble under observed (extended historical) greenhouse gas concentrations (Fig. 13b) fails however at depicting the trends for the past decades, while Euro-CORDEX (Fig. 13c) simulates an increased water availability across Germany. The future projections following the RCP8.5 scenario are roughly consistent between CMIP5 (Fig. 13d) and EURO-CORDEX (Fig. 13e). Both ensembles predict a considerable trend towards more impactful multi-year drought conditions under RCP8.5. Differences between the various sources of data may be related to specific characteristics and settings of the climate models, such as the treatment of anthropogenic aerosols, the inherited uncertainty and bias of climate models to replicate the precipitation variability at the regional and local scale, the differences of the convective precipitation during the warm part of the year (Dyrrdal et al., 2017), but also the use of multi-model ensembles that may mask the individual model skill (Ridder et al., 2022). These examples demonstrate the need for further model development to improve their ability to accurately reproduce observed CEs and their characteristics, thus reducing the uncertainty of future projections and contributing to improved prevention, risk management and future preparedness.

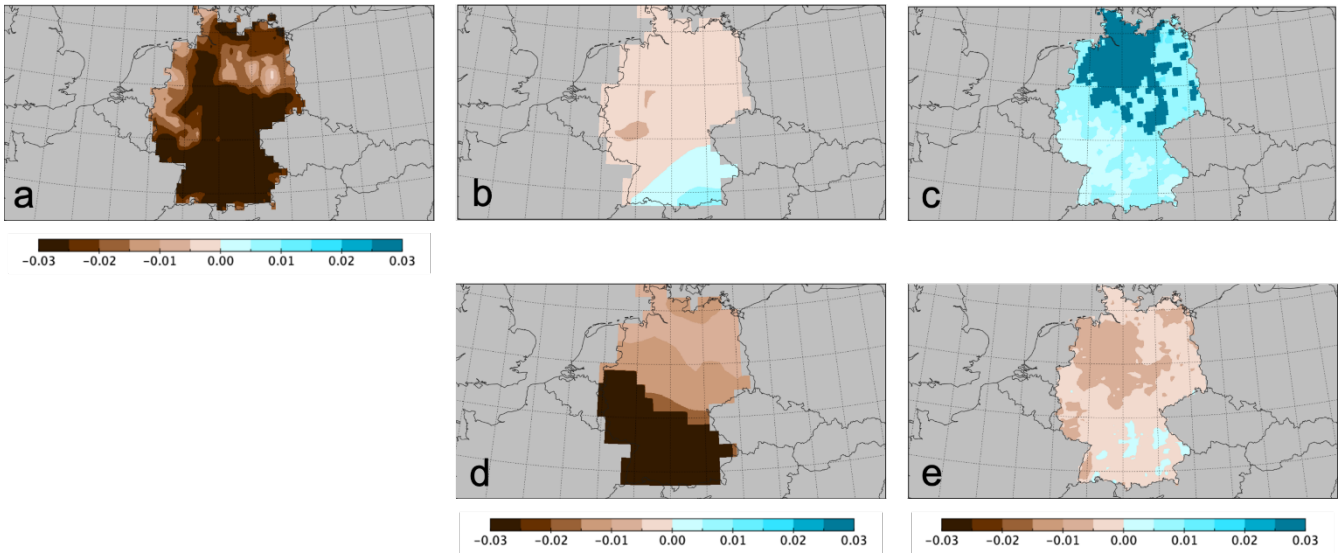

Figure 13: Decadal trends, 1975-2021 and 2022-2077, of the 3-yr running mean Standardised Precipitation Evapotranspiration Index for (a) ERA5, (b) historical CMIP5 multi-model ensemble extended by Aalbers et al. (2023), (c) EURO-CORDEX multi-model ensemble, (d) RCP8.5 CMIP5 multi-model ensemble, and (e) RCP8.5 EURO-CORDEX multi-model ensemble. Significant model ensemble grid points are shaded dark brown and dark green. Units in standard deviation for spring and summer.

5 Conclusions – Lessons learned and future steps

Compound climate events had severe impacts across Europe in 2018, as combinations of extreme weather events unfolded simultaneously or in succession, resulting in extensive socio-economic, environmental, and infrastructural damage. The study highlights two primary types of CEs: hot-dry and wet-windy, each amplifying the effects of individual weather extremes. A variety of statistical approaches and datasets have been explored and implemented, spanning different types of events and disciplines.

The summer of 2018 was marked by prolonged heatwaves and drought conditions across Europe, driven largely by persistent large-scale atmospheric blocking. Soil moisture declined sharply from spring through summer, imposing widespread stress on agriculture, forests, and water resources. These conditions led to significant agricultural losses, particularly in winter wheat yields, and imposed severe stress on European forests, resulting in large-scale forest fires and insect outbreaks.

The winter of 2018 saw a sequence of intense storms, including Friederike and Burglind, which brought strong winds and heavy precipitation, causing widespread flooding, property damage, and economic losses in multiple countries. The combination of sustained high winds and heavy precipitation further increased the risk of landslides and rockfalls, particularly in regions with saturated and thawing soils.

Projections indicate that, under progressing climate change, hot-dry events will increase in frequency and severity, while wet-windy events may retain similar frequencies but with greater intensity. Current adaptation and risk management strategies may

be insufficient, as they often focus on single-event risks and may underestimate the compound hazards posed by concurrent extremes.

This study encourages further research on compound events to improve predictive capabilities and inform adaptation strategies. Integrated climate models that better represent the complex interactions of multiple extremes are crucial. Next steps involve validating the physical relationships between predictors and CEs to identify the underlying mechanisms that drive or modify these events, which could lead to more accurate analyses and predictions of CEs. Furthermore, given the complexity of CEs and their direct impacts, a redefinition of events based primarily on their relevant impacts, rather than purely statistical characteristics, is necessary to effectively assess and manage these risks.

These findings underscore the need for comprehensive climate adaptation approaches that address the interconnected nature of compound events, ensuring more effective preparedness for the compounded risks of future climate extremes.

Code availability

Code is available from the authors upon request.

Data availability

The ERA5 (https://doi.org/10.1002/qj.3803, Hersbach et al., 2020) reanalysis data are publicly available via the Copernicus Climate Change Service (https://doi.org/10.24381/cds.adbb2d47, Hersbach et al., 2023). The gridded observational datasets E-OBS (https://doi.org/10.1029/2017JD028200, Cornes et al., 2018) are publicly available on the European Climate Assessment & Dataset website (https://www.ecad.eu/download/ensembles/download.php, ECA&D, 2023). The observational datasets (https://doi.org/10.5194/asr-10-99-2013, Kaspar et al., 2013) and the phenological data from the German Weather Service (DWD; https://doi.org/10.5194/asr-11-93-2014, Kaspar et al., 2015) are publicly available on the DWD website under their Open Data Portal (https://opendata.dwd.de/, DWD, 2023). The yield productivity data (http://dx.doi.org/10.22029/jlupub-7177, Ellsäßer and Xoplaki, 2022a), the yield anomaly catalogue (http://dx.doi.org/10.22029/jlupub-7176, Ellsäßer and Xoplaki, 2022b) and supplementary data (http://dx.doi.org/10.22029/jlupub-7203, Ellsäßer and Xoplaki, 2022c) are publicly available at the JLUpub research data repository. Historic climate data from the GSWP-W5E5 dataset used for LPJmL5 simulations are available from https://doi.org/10.48364/ISIMIP.982724 (Lange et al., 2022). The historical data of atmospheric N deposition and atmospheric CO_2 concentrations can be obtained from https://doi.org/10.48364/ISIMIP.600567 (Yang and Tian, 2020) and https://doi.org/10.48364/ISIMIP.664235.2 (Büchner and Reyer, 2022), respectively. All input data, model code, model outputs, and post-processing scripts that have been used to produce the LPJmL-related results in this paper are archived at the Potsdam Institute for Climate Impact Research and are available upon request.

Competing interests

At least one of the (co-)authors is a member of the editorial board of Natural Hazards and Earth System Sciences. The peer-review process was guided by an independent editor, and the authors also have no other competing interests to declare.

Author Contribution

EX and FE coordinated the interdisciplinary task force on compound events within climXtreme and this collaborative paper, conducted the agriculture case study analysis with Figure 6, prepared the first and final drafts of the paper based on the contribution of the co-authors; ER contributed the drivers of the hot summer of 2018 case study with Figure 1; SS contributed the detection of spatial patterns of extreme events and Figure 2; LG and SK contributed with the surface water storage case study analysis and Figure 3; LJ contributed the soil moisture case study and Figure 4; JH contributed with the analysis of the agricultural and hydrological droughts and Figure 5; DG and FK contributed with the forestry case study; JGP and T-CC contributed the windstorms description and prepared Figure 7 and S1; JGP contributed to the compound events under climate change section; JG conducted the loss analysis for windstorms with Figure 8 and contributed to the methods section; FS conducted the copula analysis and prepared Figure 9; KNM contributed the rockfall events case study analysis with Figure 10, drafted the section on precipitation-wind compound events and contributed to the compound events under climate change section; SM and MA analysed convective storms and provided Figure 11; LSG did the CMIP6 MPI-GE projection study and prepared Figure 12; KH contributed the analysis of soil moisture representation and trend in model simulations with Figure 13. NL and OV contributed to the temperature-precipitation compound events section; JL contributed drafting different sections and versions of the paper and all authors followed the analysis from the beginning, provided text and edited/commented the final version of the manuscript.

Acknowledgements

This paper is a collaborative effort within the BMBF climXtreme project, for which the authors acknowledge funding (grant numbers 01LP1901A, 01LP1903C, 01LP1901F, 01LP1903A, 01LP1902J, 01LP1903F, 01LP1902M, 01LP1901E). EX, NL, OV acknowledge support by the EU Horizon 2020 Project CLINT under Grant Agreement number 101003876. EX acknowledges support by the BMWK project DAKI-FWS (grant number 01MK21009I) and the EU Horizon Europe project MedEWSa under Grant Agreement number 101121192. JGP thanks the AXA research fund for support. LSG has also received funding from the European Union's Horizon Europe Framework Programme under the Marie Skłodowska-Curie grant agreement No 101064940. SMVB acknowledges funding from the DFG training group NatRiskChange (grant No GRK 2043/1). We acknowledge the World Climate Research Programme's Working Group on Coupled Modelling, which is responsible for CMIP, and we thank the climate modelling groups for producing and making available their model output. For CMIP the U.S. Department of Energy's Program for Climate Model Diagnosis and Intercomparison provides coordinating support and led development of software infrastructure in partnership with the Global Organization for Earth System Science Portals. We acknowledge the World Climate Research Programme's Working Group on Regional Climate, and the Working

Group on Coupled Modelling, former coordinating body of CORDEX and responsible panel for CMIP5. We also thank the climate modelling groups for producing and making available their model output. We also acknowledge the Earth System Grid Federation infrastructure, an international effort led by the U.S. Department of Energy's Program for Climate Model Diagnosis and Intercomparison, the European Network for Earth System Modelling and other partners in the Global Organisation for Earth System Science Portals (GO-ESSP). We acknowledge the E-OBS dataset from the EU-FP6 project UERRA (http://www.uerra.eu) and the Copernicus Climate Change Service, and the data providers in the ECA&D project (https://www.ecad.eu).

References

Aalbers, E. E., van Meijgaard, E., Lenderink, G., de Vries, H., and van den Hurk, B. J. J. M.: The 2018 west-central European drought projected in a warmer climate: how much drier can it get?, Nat. Hazards Earth Syst. Sci., 23, 1921–1946, https://doi.org/10.5194/nhess-23-1921-2023, 2023.

Allen, C. D., Breshears, D. D., and McDowell, N. G.: On underestimation of global vulnerability to tree mortality and forest die-off from hotter drought in the Anthropocene, Ecosphere, 6, 1-55, 2015.

Augenstein, M., Mohr, S., and Kunz, M.: Analysis of thunderstorm clusters derived from lightning data with ST-DBSCAN in West and Central Europe, Nat. Hazards Earth Syst. Sci., in prep.

Barriopedro, D., Fischer, E.M., Luterbacher, J., Trigo, R.M., and García-Herrera, R.: The hot summer of 2010: redrawing the temperature record map of Europe, Science, 332, 220-224, 2011.

Bastos, A., et al.: Direct and seasonal legacy effects of the 2018 heat wave and drought on European ecosystem productivity, Sci. Adv., 6, eaba2724, https://doi.org/10.1126/sciadv.aba2724, 2020.

Bastos, A., Orth, R., Reichstein, M., Ciais, P., Viovy, N., et al.: Vulnerability of European ecosystems to two compound dry and hot summers in 2018 and 2019, Earth Syst. Dyn., 12:1015–1035, 2021, https://doi.org/10.5194/esd-12-1015-2021

Beloiu, M., Stahlmann, R., and Beierkuhnlein, C.: High Recovery of Saplings after Severe Drought in Temperate Deciduous Forests, Forests, 11:546, https://doi.org/10.3390/f11050546, 2020.

Beillouin, D., Schauberger, B., Bastos, A., Ciais, P., and Makowski, D.: Impact of extreme weather conditions on European crop production in 2018, Philos. T. R. Soc. B, 375, 20190510, https://doi.org/10.1098/rstb.2019.0510, 2020.

Bender, J.: Zur Ermittlung von hydrologischen Bemessungsgrößen an Flussmündungen mit Verfahren der multivariaten Statistik. Mitteilung des Forschungsinstituts Wasser und Umwelt der Universität Siegen, 9. http://dokumentix.ub.uni-siegen.de/opus/volltexte/2015/965/pdf/Dissertation_Jens_Bender.pdf, 2015.

Bevacqua, E., De Michele, C., Manning, C., Couasnon, A., Ribeiro, A. F. S., Ramos, A. M., et al.: Guidelines for studying diverse types of compound weather and climate events, Earth's Future, 9:e2021EF002340, https://doi.org/10.1029/2021EF002340, 2021.

Bevacqua, E., Maraun, D., Hobæk Haff, I., Widmann, M., and Vrac, M.: Multivariate statistical modelling of compound events via pair-copula constructions: analysis of floods in Ravenna (Italy), Hydrol. Earth Syst. Sci., 21, 2701–2723. https://doi.org/10.5194/hess-21-2701-2017, 2017.

Bevacqua, E., Suarez-Gutierrez, L., Jézéquel, A., Lehner, F., Vrac, M., Yiou, P., and Zscheischler J.: Advancing research on compound weather and climate events via large ensemble model simulations, Nat. Commun., 14, 2145, https://doi.org/10.1038/s41467-023-37847-5, 2023.

Birant, D., and Kut, A.: ST-DBSCAN: An algorithm for clustering spatial-temporal data. Data Know. Eng., 60, 208-221, https://doi.org/10.1016/j.datak.2006.01.013, 2007.

Blauhut, V., Stoelzle, M., Ahopelto, L., Brunner, M. I., Teutschbein, C., Wendt, D. E., Akstinas, V., Bakke, S. J., Barker, L. J., Bartošová, L., Briede, A., Cammalleri, C., Kalin, K. C., De Stefano, L., Fendeková, M., Finger, D. C., Huysmans, M., Ivanov, M., Jaagus, J., Jakubínský, J., Krakovska, S., Laaha, G., Lakatos, M., Manevski, K., Neumann Andersen, M., Nikolova, N., Osuch, M., van Oel, P., Radeva, K., Romanowicz, R. J., Toth, E., Trnka, M., Urošev, M., Urquijo Reguera, J., Sauquet, E., Stevkov, A., Tallaksen, L. M., Trofimova, I., Van Loon, A. F., van Vliet, M. T. H., Vidal, J.-P., Wanders, N., Werner, M., Willems, P., and Živković, N.: Lessons from the 2018–2019 European droughts: a collective need for unifying drought risk management, Nat. Hazards Earth Syst. Sci., 22, 2201–2217, https://doi.org/10.5194/nhess-22-2201-2022, 2022.

Brakkee, E., van Huijgevoort, M. H. J., and Bartholomeus, R. P.: Improved understanding of regional groundwater drought development through time series modelling: the 2018–2019 drought in the Netherlands, Hyd. Earth Sys. Sci., 26, 551–569. https://doi.org/10.5194/hess-26-551-2022, 2022.

Brauns, B., Cuba, D., Bloomfield, J. P., Hannah, D. M., Jackson, C., Marchant, B. P., et al.: The Groundwater Drought Initiative (GDI): Analysing and understanding groundwater drought across Europe, Proc. Int. Assoc. Hydrol. Sci., 383, 297–305. https://doi.org/10.5194/piahs-383-297-2020, 2020.

Brun, P., Psomas, A., Ginzler, C., Thuiller, W., Zappa, M., and Zimmermann, N. E.: Large-scale early-wilting response of Central European forests to the 2018 extreme drought, Glob. Change Biol., 26, 7021-7035, 2020.

Büchner, M., and Reyer, C.: ISIMIP3a atmospheric composition input data (v1.2). ISIMIP Repository. https://doi.org/10.48364/ISIMIP.664235.2, 2022

Bundesministerium für Ernährung und Landwirtschaft (BMEL): Ergebnisse der Waldzustandserhebung 2020, https://www.bmel.de/SharedDocs/Downloads/DE/_Wald/ergebnisse-waldzustandserhebung-2020.html, 2021, (Accessed 19 October 2024)

Buras, A., Rammig, A., and Zang, C. S.: Quantifying impacts of the 2018 drought on European ecosystems in comparison to 2003, Biogeosciences, 17, 1655-1672, 2020.

Caldeira, M.C., Lecomte, X., David, T.S., Pinto, J.G., Bugalho, M.N., and Werner, C.: Synergy of extreme drought and plant invasion reduce ecosystem functioning and resilience. Sci. Reports, 5,15110 https://doi.org/10.1038/srep15110, 2015

Carnicer, J., Alegria, A., Giannakopoulos, C. et al.: Global warming is shifting the relationships between fire weather and realized fire-induced CO2 emissions in Europe, Sci. Rep., 12, 10365, https://doi.org/10.1038/s41598-022-14480-8, 2022

Cerlini, P. B., Silvestri, L., Meniconi, S., and Brunone, B.: Simulation of the Water Table Elevation in Shallow Unconfined Aquifers by means of the ERA5 Soil Moisture Dataset: The Umbria Region Case Study, Earth Inter., 25, 15–32. https://doi.org/10.1175/EI-D-20-0011.1, 2021.

Conradt, T., Engelhardt, H., Menz, C. et al.: Cross-sectoral impacts of the 2018–2019 Central European drought and climate resilience in the German part of the Elbe River basin, Reg. Environ. Change, 23, https://doi.org/10.1007/s10113-023-02032-3, 2023.

Cornes, R.C., van der Schrier, G., van den Besselaar, E.J.M., and Jones, P.D.: An Ensemble Version of the E-OBS Temperature and Precipitation Data Sets, J. Geophys. Res. Atmospheres 123, 9391–9409. https://doi.org/10.1029/2017JD028200, 2018.

Cooley, D., and Thibaud, E.: Decompositions of dependence for high-dimensional extremes, Biometrika, 106, 587-604, 2019.

Cucchi, M., Weedon, G. P., Amici, A., Bellouin, N., Lange, S., Müller Schmied, H., Hersbach, H., and Buontempo, C.: WFDE5: bias-adjusted ERA5 reanalysis data for impact studies, Earth Sys. Sci. Data, 12, 2097–2120. https://doi.org/10.5194/essd-12-2097-2020, 2020.

Di Capua, G., Sparrow, S., Kornhuber, K., Rousi, E., Osprey, S., Wallom, D., van den Hurk, B. and Coumou, D.: Drivers behind the summer 2010 wave train leading to Russian heatwave and Pakistan flooding, npj Clim. Atmos. Sci., 4, 55, https://doi.org/10.1038/s41612-021-00211-9, 2021.

D'Agostino, V.: Drought in Europe summer 2018: Crisis management in an orderly chaos, Farm-Europe, https://www.farm-europe.eu/blog-en/drought-in-europe-summer-2018-crisis-management-in-an-orderly-chaos/, 2018, (Accessed 19 October 2024).

D'Amato, J., Hantz, D., Guerin, A., Jaboyedoff, M., Baillet, L., and Mariscal, A.: Influence of meteorological factors on rockfall occurrence in a middle mountain limestone cliff, Nat. Hazards Earth Syst. Sci., 16, 719–735, https://doi.org/10.5194/nhess-16-719-2016, 2016.

Dacre, H.F., Hawcroft, M.K., Stringer, M.A. and Hodges, K.I.: An extratropical cyclone database: A tool for illustrating cyclone structure and evolution characteristics, Bull. Amer. Meteorol. Soc., 93, 1497-1502, https://doi.org/10.1175/BAMS-D-11-00164.1, 2012.

de Brito, M., Kuhlicke, C. and Marx, A.: Near-real-time drought impact assessment: a text mining approach on the 2018/19 drought in Germany, Environ. Res. Lett., 15, 1040a9, 2020.

Drouard, M., Kornhuber, K., and Woollings, T.: Disentangling dynamic contributions to summer 2018 anomalous weather over Europe, Geophys. Res. Lett., 46, 12537– 12546, 2019.

Dyrrdal, A.V., Stordal, F., Lussana, C.: Evaluation of summer precipitation from EURO-CORDEX fine-scale RCM simulations over Norway, Int. J. Clim., 38, 1661-1677, https://doi.org/10.1002/joc.5287, 2017

Eisenstein, L., Schulz, B., Qadir, G. A., Pinto, J. G. and Knippertz, P.: Identification of high-wind features within extratropical cyclones using a probabilistic random forest – Part 1: Method and case studies, Weather Clim. Dynam., 3, 1157–1182, https://doi.org/10.5194/wcd-3-1157-2022, 2022.

Ellsäßer, F. and Xoplaki, E.: Cropdata – spatial yield productivity data base for the ten most cultivated crops in Germany from 1989 to 2020 - version 1.0. http://dx.doi.org/10.22029/jlupub-7177, 2022a.

Ellsäßer, F. and Xoplaki, E.: Cropdata – yield anomaly catalogue for the ten most cultivated crops in Germany from 1989 to 2020 - version 1.0. http://dx.doi.org/10.22029/jlupub-7176, 2022b.

Ellsäßer, F. and Xoplaki, E.: Cropdata – supplementary data (for spatial yield productivity data base for the ten most cultivated crops in Germany from 1989 to 2020) - version 1.0. http://dx.doi.org/10.22029/jlupub-7203, 2022c.

Ellsäßer, F. and Xoplaki, E. (in review): A unique high-resolution open access crop yield database for Germany covering the period 1989 to 2020, Scientific Data, 2024.

Ester, M., Kriegel, H.P. Sander, J., Xu, X., Simoudis, E., Han, J., and Fayyad, U.M. (eds.): A density-based algorithm for discovering clusters in large spatial databases with noise. Proceedings of the Second International Conference on Knowledge Discovery and Data Mining (KDD-96). AAAI Press. pp. 226–231. CiteSeerX 10.1.1.121.9220. ISBN 1-57735-004-9, 1996

Feurdean, A., Vannière, B., Finsinger, W., Warren, D., Connor, S.C., Forrest, M., Liakka, J., et al.: Fire hazard modulation by long-term dynamics in land cover and dominant forest type in eastern and central Europe, Biogeosciences, 17, 1213–1230, 2020.

Fischer, E. M., Seneviratne, S. I., Vidale, P. L., Lüthi, D., and Schär, C.: Soil moisture—atmosphere interactions during the 2003 European summer heatwave, J. Clim., 20: 5081–5099, 2007.

Fischer, E. M., and Schär, C.: Consistent geographical patterns of changes in high-impact European heatwaves, Nat. Geosci., 3, 398–403, https://doi.org/10.1038/ngeo866, 2010.

Fink, A. H., Brücher, T., Krüger, A., Leckebusch, G. C., Pinto, J. G. and Ulbrich, U.: The 2003 European summer heatwaves and drought –synoptic diagnosis and impacts, Weather, 59, 209–216, https://doi.org/10.1256/wea.73.04, 2004.

Fink, A. H., Brücher, T., Ermert, V., Krüger, A., and Pinto, J. G.: The European storm Kyrill in January 2007: synoptic evolution, meteorological impacts and some considerations with respect to climate change, Nat. Hazards Earth Syst. Sci., 9, 405–423, https://doi.org/10.5194/nhess-9-405-2009, 2009.

Frank, M.J.: On the simultaneous associativity of F(x,y) and x+y-F(x,y), Aequationes Mathematicae, 19, 194-226, 1979.

Furusho-Percot, C., Goergen, K., Hartick, C., Kulkarni, K., Keune, J., and Kollet, S.: Pan-European groundwater to atmosphere terrestrial systems climatology from a physically consistent simulation, Sci. Data., 6. https://doi.org/10.1038/s41597-019-0328-7, 2019.

García-Herrera, R., Díaz, J., Trigo, R.M., Luterbacher, J., and Fischer, E. M.: A Review of the European Summer Heat Wave of 2003, Crit. Rev. Env. Sci. Tech., 40, 267-306, https://doi.org/10.1080/10643380802238137, 2010.

Giorgi, F., Jones, C., and Arsar, G. R.: Addressing climate information needs at the regional level: the CORDEX framework, WMO Bulletin, 58, 175-183, 2009.

Hari, V., Rakovec, O., Markonis, Y., Hanel, M., and Kumar, R.: Increased future occurrences of the exceptional 2018–2019 Central European drought under global warming, Sci. Rep., 10, 1-10, 2020.

Hartick, C., Furusho-Percot, C., Goergen, K., & Kollet, S.: An interannual probabilistic assessment of subsurface water storage over Europe using a fully coupled terrestrial model, Wat. Res. Res., 57, e2020WR027828, 2021.

Hersbach, H., and Coauthors: The ERA5 global reanalysis, Q.J.R. Meteorol. Soc., 146, 1999-2049, https://doi.org/10.1002/qj.3803, 2020.

Hersbach, H., Bell, B., Berrisford, P., Biavati, G., Horányi, A., Muñoz Sabater, J., Nicolas, J., Peubey, C., Radu, R., Rozum, I., Schepers, D., Simmons, A., Soci, C., Dee, D., and Thépaut, J-N.: ERA5 hourly data on single levels from 1940 to present. Copernicus Climate Change Service (C3S) Climate Data Store (CDS), https://doi.org/10.24381/cds.adbb2d47, 2023.

Hlásny, T., Zimová, S., Merganičová, K., Štěpánek, P., Modlinger, R., and Turčáni, M: Devastating outbreak of bark beetles in the Czech Republic: Drivers, impacts, and management implications, For. Ecol. Manage., 490, https://doi.org/10.1016/j.foreco.2021.119075, 2021.

Herzfeld, T., Heinke, J., Rolinski, S., and Müller, C.: Soil organic carbon dynamics from agricultural management practices under climate change, Earth Sys. Dyn., 12, 1037–1055, https://doi.org/10.5194/esd-12-1037-2021, 2021.

IPCC: Impacts, Adaptation, and Vulnerability. Contribution of Working Group II to the Sixth Assessment Report of the Intergovernmental Panel on Climate Change [H.-O. Pörtner, D.C. Roberts, M. Tignor, E.S. Poloczanska, K. Mintenbeck, A. Alegría, M. Craig, S. Langsdorf, S. Löschke, V. Möller, A. Okem, B. Rama (eds.)]. Cambridge University Press. Cambridge University Press, Cambridge, UK and New York, NY, USA, 3056 pp., https://doi.org/10.1017/9781009325844, 2022

Jane, R., Cadavid, L., Obeysekera, J., Wahl, T.: Multivariate statistical modelling of the drivers of compound flood events in south Florida. Nat. Hazards Earth Syst. Sci. 20, 2681–2699, https://doi.org/10.5194/nhess-20-2681-2020, 2020

Kaiser, D., Voynova, Y.G., and Brix, H.: Effects of the 2018 European heatwave and drought on coastal biogeochemistry in the German Bight, Sci. Tot. Environ., 892, 164316, https://doi.org/10.1016/j.scitotenv.2023.164316, 2023

Kaspar, F., Friedrich, K., and Imbery, F.: Observed temperature trends in Germany: Current status and communication tools, Meteorol. Z. (Contrib. Atm. Sci.), https://doi.org/10.1127/metz/2023/1150, 2023.

Kaspar, F., Müller-Westermeier, G., Penda, E., Mächel, H., Zimmermann, K., Kaiser-Weiss, A., and Deutschländer, T.: Monitoring of climate change in Germany – data, products and services of Germany's National Climate Data Centre, Adv. Sci. Res., 10, 99–106, https://doi.org/10.5194/asr-10-99-2013, 2013.

Kaspar, F., Zimmermann, K., and Polte-Rudolf, C.: An overview of the phenological observation network and the phenological database of Germany's national meteorological service (Deutscher Wetterdienst), Adv. Sci. Res., 11, 93–99, 2015.

Kautz, L.A., Martius, O., Pfahl, S., Pinto, J.G., Ramos, A.M., Sousa, P.M., and Woollings, T.: Atmospheric Blocking and Weather Extremes over the Euro-Atlantic Sector - A Review, Weather Clim. Dynam. 3, 305-336, https://doi.org/10.5194/wcd-3-305-2022, 2022

Kendall, M.G.: Rank correlation methods. 4 ed., 2. Impr. London: Griffin. ISBN 0852641990, 1975.

Kim, H.: Global Soil Wetness Project Phase 3 Atmospheric Boundary Conditions (Experiment 1) [Data set]. Data Integration and Analysis System (DIAS), https://doi.org/10.20783/DIAS.501, 2017.

Kohonen, T.: Essentials of the self-organizing map, Neural Networks, 37, 52–65, https://doi.org/10.1016/j.neunet.2012.09.018, 2013.

Kornhuber, K., Osprey, S., Coumou, D., Petri, S., Petoukhov, V., Rahmstorf, S. and Gray, L.: Extreme weather events in early Summer 2018 connected by a recurrent hemispheric wave pattern, Environ. Res. Lett., 14, 054002, https://doi.org/10.31223/osf.io/tq23m, 2019.

Kornhuber, K., Coumou, D., Vogel, E., Lesk, C., Donges, J. F., Lehmann, J. and Horton, R. M.: Amplified Rossby waves enhance risk of concurrent heatwaves in major breadbasket regions, Nat. Clim. Chang., 10, 48–53, https://doi.org/10.1038/s41558-019-0637-z, 2020.

Lange, S., Mengel, M., Treu, S., and Büchner, M.: ISIMIP3a atmospheric climate input data (v1.0), ISIMIP Repository, https://doi.org/10.48364/ISIMIP.982724, 2022.

Leonard, M., Westra, S., Phatak, A., Lambert, M., van den Hurk, B., McInnes, K., Risbey, J., Schuster, S., Jakob, D., and Stafford-Smith, M.: A compound event framework for understanding extreme impacts, WIRES. Clim. Change, 5, 113–128, https://doi.org/10.1002/wcc.252, 2014.

Leuschner, C.: Drought response of European beech (Fagus sylvatica L.) – a review, Persp. Plant Ecol., Evol. and Syst., 47, 125576, https://doi.org/10.1016/j.ppees.2020.125576, 2020.

Lidskog, R., Johansson, J., and Sjödin, D.: Wildfires, responsibility and trust: public understanding of Sweden'largest wildfire, Scand. J. For. Res., 34, 319-328, 2019.

Liu, Xuebang, et al.: Similarities and differences in the mechanisms causing the European summer heatwaves in 2003, 2010, and 2018, Earth's Future, 7, e2019EF001386, https://doi.org/10.1029/2019EF001386, 2020.

Lorenz, R., Jaeger, E. B., and Seneviratne, S. I.: Persistence of heat waves and its link to soil moisture memory, Geophys. Res. Lett., 37, L09703, 2010.

Lutz, F., Herzfeld, T., Heinke, J., Rolinski, S., Schaphoff, S., von Bloh, W., Stoorvogel, J. J. J., and Müller, C.: Simulating the effect of tillage practices with the global ecosystem model LPJmL (version 5.0-tillage), Geosci. Mod. Develop., 12, 2419–2440. https://doi.org/10.5194/gmd-12-2419-2019, 2019.

Luterbacher, J., Dietrich, D., Xoplaki, E., Grosjean, M. and Wanner, H.: European seasonal and annual temperature variability, trends and extremes since 1500, Science, 303: 1499–1503, 2004.

Manning, C., Widmann, M., Bevacqua, E., Van Loon, A. F., Maraun, D., and Vrac, M.: Soil moisture drought in Europe: a compound event of precipitation and potential evapotranspiration on multiple time scales, J. Hydrometeorol., 19, 1255–1271, https://doi.org/10.1175/JHM-D-18-0017.1, 2018.

Manning, C., Widmann, M., Maraun, D., Van Loon, A. F., and Bevacqua, E.: Large spread in the representation of compound long-duration dry and hot spells over Europe in CMIP5, Weather Clim. Dynam., 4, 309–329, https://doi.org/10.5194/wcd-4-309-2023, 2023.

Manning, C., Kendon, E.J., Fowler, H.J., Catto, J.F., Chan, S.C., and Sansom, P.G.: Compound wind and rainfall extremes: Drivers and future changes over the UK and Ireland, Wea. and Clim. Extremes, 44, 100673, https://doi.org/10.1016/j.wace.2024.100673, 2024

McKee, T. B., Doesken, N. J., and Kleist, J.: The relationship of drought frequency and duration to time scales, Eighth Conference on Appl. Climatol., 179–184, 1993.

Martius, O.; Pfahl, S. and Chevalier, C.: A global quantification of compound precipitation and wind extremes, Geophys. Res. Lett., 43, 7709–7717, https://doi.org/10.1002/2016GL070017, 2016.

Matzarakis, A., Laschewski, G., and Muthers, S.: The Heat Health Warning System in Germany—Application and Warnings for 2005 to 2019, Atmosphere, 11, 170, https://doi.org/10.3390/atmos11020170, 2020.

Messmer, M. and Simmonds, I.: Global analysis of cyclone-induced compound precipitation and wind extreme events, Weath. Clim. Extremes, 32, 100324, 2021.

Milanovic, S., Markovic, N., Pamucar, D., Gigovic, L., Kostic, P. and Milanovic, S.D.: Forest Fire Probability Mapping in Eastern Serbia: Logistic Regression versus Random Forest Method, Forests. 12: 5, https://doi.org/10.3390/f12010005, 2021.

Miralles, D.G., Gentine, P., Seneviratne, S.I. and Teuling, A.J.: Land–atmospheric feedbacks during droughts and heatwaves: state of the science and current challenges, Ann. N.Y. Acad. Sci., 1436: 19-35, https://doi.org/10.1111/nyas.13912, 2019

Mohr, S., Wandel, J., Lenggenhager, S., and Martius, O.:Relationship between atmospheric blocking and warm season thunderstorms over western and central Europe, Q. J. Roy. Meteor. Soc., 145, 3040–3056, https://doi.org/10.1002/qj.3603, 2019.

Mohr, S., Wilhelm, J., Wandel, J., Kunz, M., Portmann, R., Punge, H. J., Schmidberger, M., Quinting, J. F., and Grams, C.: The role of large-scale dynamics in an exceptional sequence of severe thunderstorms in Europe May/June 2018, Weather Clim. Dynam., 1, 325–348, https://doi.org/10.5194/wcd-1-325-2020, 2020.

Deutscher Wetterdienst, 2018: Monatlicher Klimastatus Deutschland August 2018. DWD, Geschäftsbereich Klima und Umwelt, Offenbach, 29 Seiten, www.dwd.de/DE/derdwd/bibliothek/fachpublikationen/selbstverlag/selbstverlag_node.html (Accessed: 19th October 2024).

Munich RE, Extreme storms, wildfires and droughts cause heavy nat cat losses in 2018. 08/01/2019 Media Information, available at: https://www.munichre.com/en/company/media-relations/media-information-and-corporate-news/media-information/2019/2019-01-08-media-information.html, 2019.

Naturgefahrenreport 2019, Die Schaden-Chronik der deutschen Versicherer, Gesamtverband der Deutschen Versicherungswirtschaft, 56 pages e. V., https://www.gdv.de/resource/blob/51710/e5eaa53a9ec21fb9241120c1d1850483/naturgefahrenreport-2019-schaden-chronik-data.pdf (Accessed 19 October 2024).

Nissen, K. M., Rupp, S., Kreuzer, T. M., Guse, B., Damm, B., and Ulbrich, U.: Quantification of meteorological conditions for rockfall triggers in Germany, Nat. Hazards Earth Syst. Sci., 22, 2117–2130, https://doi.org/10.5194/nhess-22-2117-2022, 2022.

Nogueira, M.: Inter-comparison of ERA-5, ERA-Interim and GPCP rainfall over the last 40 years: process-based analysis of systematic and random differences, J. Hydrol., 583, 124632, https://doi.org/10.1016/j.jhydrol.2020.124632, 2020.

OECD.: Managing Climate Risks, Facing up to Losses and Damages, OECD Publishing, Paris, https://doi.org/10.1787/55ea1cc9-en, 2021.

Öhrn, P., Berlin, M., Elfstrand, M., Krokene, P., and Jönsson, A. M.: Seasonal variation in Norway spruce response to inoculation with bark beetle-associated bluestain fungi one year after a severe drought, For. Ecol. Manage., 496, 119443, 2021.

Olonscheck, D., Suarez-Gutierrez, L., Milinski, S., et al.: The new Max Planck Institute Grand Ensemble with CMIP6 forcing and high-frequency model output, Authorea, https://doi.org/10.22541/essoar.168319746.64037439/v1, May 4, 2023.

Orth, R., and Seneviratne, S. I.: Analysis of soil moisture memory from observations in Europe, J. Geophys. Res., 117, D15115, https://doi.org/10.1029/2011JD017366, 2012.

Pinto, J. G., Spangehl, T., Ulbrich, U., and Speth, P.: Sensitivities of a cyclone detection and tracking algorithm: individual tracks and climatology, Met. Zeitschrift, 14, 823 – 838, https://doi.org/10.1127/0941-2948/2005/0068, 2005.

Pinto, J. G., Zacharias, S., Fink, A.H., Leckebusch, G.C, and Ulbrich, U.: Factors contributing to the development of extreme North Atlantic cyclones and their relationship with the NAO, Clim. Dynam., 32, 711–737, https://doi.org/10.1007/s00382-008-0396-4, 2009.

Piper, D., Kunz, M., Ehmele, F., Mohr, S., Mühr, B., Kron, A., and Daniell, J.: Exceptional sequence of severe thunderstorms and related flash floods in May and June 2016 in Germany – Part 1: Meteorological background, Nat. Hazards Earth Syst. Sci., 16, 2835–2850, https://doi.org/10.5194/nhess-16-2835-2016, 2016.

Piper, D. A., Kunz, M., Allen, J. T., and Mohr, S.: Investigation of the temporal variability of thunderstorms in Central and Western Europe and the relation to large-scale flow and teleconnection patterns, Q. J. Roy. Meteor. Soc., 145, 3644–3666, https://doi.org/10.1002/qj.3647, 2019.

Rauthe, M., Steiner, H., Riediger, U., Mazurkiewicz, A., and Gratzki, A.: A Central European precipitation climatology – Part I: Generation and validation of a high-resolution gridded daily data set (HYRAS), Meteorol. Z., 22, 235–256, https://doi.org/10.1127/0941-2948/2013/0436, 2013.

Raymond, C., Horton, R.M., Zscheischler, J., Martius, O., AghaKouchak, A., Balch, J., Bowen, S. G., Camargo, S. J., Hess, J., Kornhuber, K., Oppenheimer, M., Ruane, A. C., Wahl, T., and White, K.: Understanding and managing connected extreme events, Nat. Clim. Chang., 10, 611–621, https://doi.org/10.1038/s41558-020-0790-4, 2020.

Resnick, S. I.: Heavy-tail phenomena: probabilistic and statistical modelling, Springer Science & Business Media, 2007.

Riahi, K., van Vuuren, D.P., et al.: The Shared Socioeconomic Pathways and their energy, land use, and greenhouse gas emissions implications: An overview, Glob. Environ. Change, 42, 153-168, https://doi.org/10.1016/j.gloenvcha.2016.05.009, 2017.

Ridder, N., Pitman, A. J., Westra, S., Ukkola, A., Do, H., Bador, M., et al.: Global hotspots for the occurrence of compound events, Nat. Comm., 11, 5956, https://doi.org/10.1038/s41467-020-19639-3, 2020.

Ridder, N. N., Pitman, A. J., & Ukkola, A. M.: Do CMIP6 climate models simulate global or regional compound events skillfully?, Geophys. Res. Lett. 48, e2020GL091152, https://doi.org/10.1029/2020GL091152, 2021.

Ridder, N.N., Ukkola, A.M., Pitman, A.J. et al.: Increased occurrence of high impact compound events under climate change, npj Clim. Atmos. Sci., 5, 3, https://doi.org/10.1038/s41612-021-00224-4, 2022.

Rösner, B. et al., The long heat wave and drought in Europe in 2018 [in “State of the Climate in 2018”], Bull. Am. Meteorol. Soc., 100, S222–S223, https://doi.org/10.1175/2019BAMSStateoftheClimate.1, 2019

Rupp S. and Damm, B.: A national rockfall dataset as a tool for analysing the spatial and temporal rockfall occurrence in Germany, Earth Surf. Process. Landforms, 45, 1528–1538, https://doi.org/10.1002/esp.4827, 2020.

Rousi, E., Anagnostopoulou, C., Tolika, K. and Maheras, P.: Representing teleconnection patterns over Europe: A comparison of SOM and PCA methods, Atmos. Res., 152, 123–137, https://doi.org/10.1016/j.atmosres.2013.11.010, 2015.

Rousi, E., Kornhuber, K., Beobide-Arsuaga, G. et al.: Accelerated western European heatwave trends linked to more-persistent double jets over Eurasia, Nat. Commun., 13, 3851, https://doi.org/10.1038/s41467-022-31432-y, 2022.

Rousi, E., Fink, A. H., Andersen, L. S., Becker, F. N., Beobide-Arsuaga, G., Breil, M., Cozzi, G., Heinke, J., Jach, L., Niermann, D., Petrovic, D., Richling, A., Riebold, J., Steidl, S., Suarez-Gutierrez, L., Tradowsky, J. S., Coumou, D., Düsterhus, A., Ellsäßer, F., Fragkoulidis, G., Gliksman, D., Handorf, D., Haustein, K., Kornhuber, K., Kunstmann, H., Pinto, J. G., Warrach-Sagi, K., and Xoplaki, E.: The extremely hot and dry 2018 summer in central and northern Europe from a multi-faceted weather and climate perspective, Nat. Hazards Earth Syst. Sci., 23, 1699–1718, https://doi.org/10.5194/nhess-23-1699-2023, 2023.

Schaphoff, S., von Bloh, W., Rammig, A., Thonicke, K., Biemans, H., Forkel, M., Gerten, D., Heinke, J., Jägermeyr, J., Knauer, J., Langerwisch, F., Lucht, W., Müller, C., Rolinski, S., Waha, K., Knauer, J., von Bloh, W., Gerten, D., Jägermeyr, J., and Waha, K.: LPJmL4 – a dynamic global vegetation model with managed land – Part 1: Model description, Geosci. Mod. Develop. 11, 1343–1375, https://doi.org/10.5194/gmd-11-1343-2018, 2018.

Schuldt, B., Knutzen, F., Delzon, S., Jansen, S., Müller-Haubold, H., Burlett, R., and Leuschner, C.: How adaptable is the hydraulic system of European beech in the face of climate change-related precipitation reduction?, New Phytol., 210, 443-458, 2016.

Schuldt, B., Buras, A., Arend, M., Vitasse, Y., Beierkuhnlein, C., Damm, A., and Kahmen, A.: A first assessment of the impact of the extreme 2018 summer drought on Central European forests, Basic Appl. Ecol. 45, 86-103, 2020.

Schulz, W., Diendorfer, G., Pedeboy, S., and Poelman, D.R.: The European lightning location system EUCLID – Part 1: Performance analysis and validation, Nat. Hazards Earth Syst. Sci., 16, 595–605, https://doi.org/10.5194/nhess-16-595-2016, 2016.

Seneviratne, S. I., et al.: Changes in climate extremes and their impacts on the natural physical environment. Managing the Risks of Extreme Events and Disasters to Advance Climate Change Adaptation, C. B. Field et al., Eds., Cambridge University Press, 109–230, 2012.

Seneviratne, S.I., et al.: The Physical Science Basis. Contribution of Working Group I to the Sixth Assessment Report of the Intergovernmental Panel on Climate Change [Masson-Delmotte, V., P. Zhai, A. Pirani, S.L. Connors, C. Péan, S. Berger, N. Caud, Y. Chen, L. Goldfarb, M.I. Gomis, M. Huang, K. Leitzell, E. Lonnoy, J.B.R. Matthews, T.K. Maycock, T. Waterfield, O. Yelekçi, R. Yu, and B. Zhou (eds.)]. Cambridge University Press, Cambridge, United Kingdom and New York, NY, USA, pp. 1513–1766, https://doi.org/10.1017/9781009157896.013, 2021.

Senf, C., and Seidl, R.: Persistent impacts of the 2018 drought on forest disturbance regimes in Europe, Biogeosci., 18, 5223-5230, 2021.

Shyrokaya, A. et al.: Significant relationships between drought indicators and impacts for the 2018–2019 drought in Germany, Environ. Res. Lett. 19 014037, 2024, DOI 10.1088/1748-9326/ad10d9

Simpson, N.P., et al.: A framework for complex climate change risk assessment, One Earth, 4, 489–501, https://doi.org/10.1016/j.oneear.2021.03.005, 2021.

Statistische Ämter des Bundes und der Länder. Regionaldatenbank Deutschland, https://www.regionalstatistik.de/genesis/online/logon, 2021 (Accessed 19 October 2024).

Song, Y.M., Wang, Z.F., Qi, L.L., and Huang, A.N.: Soil Moisture Memory and Its Effect on the Surface Water and Heat Fluxes on Seasonal and Interannual Time Scales, J. Geophys. Res. Atmos., 124, 10730–10741, 2019.

Sousa, P. M., et al.: Distinct influences of large-scale circulation and regional feedbacks in two exceptional 2019 European heatwaves, Commun. Earth Environ., 1, 48, https://doi.org/10.1038/s43247-020-00048-9, 2020.

Spensberger, C., Madonna, E., Boettcher, M., Grams, C. M., Papritz, L., Quinting, J. F., Röthlisberger, M., Sprenger, M. and Zschenderlein, P.: Dynamics of concurrent and sequential Central European and Scandinavian heatwaves, Q. J. R. Meteorol. Soc., 146, 2998–3013, https://doi.org/10.1002/QJ.3822, 2020.

Stefanon, M., D'Andrea, F. and Drobinski, P.: Heatwave classification over Europe and the Mediterranean region, Environ. Res. Lett., 7, 014023, https://doi.org/10.1088/1748-9326/7/1/014023, 2012.

Szemkus S., and Friederichs P.: "Spatial patterns and indices for heat waves and droughts over Europe using a decomposition of extremal dependency". Advances in Statistical Climatology, Meteorology and Oceanography 10.1, https://doi.org/10.5194/ascmo-10-29-2024, 2024.

Taylor, K.E., Stouffer, R.J., and Meehl, G.A.: An Overview of CMIP5 and the experiment design, Bull. Amer. Meteor. Soc., 93, 485-498, https://doi.org/10.1175/BAMS-D-11-00094.1, 2012.

Tijdeman, E., and Menzel, L.: The development and persistence of soil moisture stress during drought across southwestern Germany, Hydrol. and Earth Sys. Sci., 25, 2009–2025, https://doi.org/10.5194/hess-25-2009-2021, 2021.

Toreti, A., Belward, A., Perez-Dominguez, I., Naumann, G., Luterbacher, J., Cronie, O., Seguini, L., Manfron, G., Lopez-Lozano, R., Baruth, B., Berg, M., Dentener, F., Ceglar, A., Chatzopoulos, T., and Zampieri, M.: The Exceptional 2018 European Water Seesaw Calls for Action on Adaptation, Earth's Future 7, 652–663, https://doi.org/10.1029/2019EF001170, 2019a.

Toreti, A., Cronie, O. & Zampieri, M. Concurrent climate extremes in the key wheat producing regions of the world, Sci. Rep., 9, 5493, https://doi.org/10.1038/s41598-019-41932-5 , 2019b.

UNFCCC: Loss and Damage, online guide, United Nations Framework Convention on Climate Change, 46 pages, https://unfccc.int/sites/default/files/resource/loss_and_damage_online_guide.pdf, 2024 (Accessed 19 October 2024).

van Delden, A.: The synoptic setting of thunderstorms in western Europe, Atmos. Res., 56, 89–110, https://doi.org/10.1016/S0169-8095(00)00092-2, 2001.

van der Wiel, K., Lenderink, G., and de Vries, H.: Physical storylines of future European drought events like 2018 based on ensemble climate modelling, Weath. Clim. Extremes, 33, 100350, https://doi.org/10.1016/j.wace.2021.100350, 2021.

Van Loon, A. F., and Van Lanen, H. A. J.: A process-based typology of hydrological drought. Hydrol. Earth Syst. Sci., 16, 1915–1946, https://doi.org/10.5194/hess-16-1915-2012, 2012.

Vautard, R., van Oldenborgh, G. J., Otto, F. E. L., Yiou, P., de Vries, H., van Meijgaard, E., Stepek, A., Soubeyroux, J.-M., Philip, S., Kew, S. F., Costella, C., Singh, R., and Tebaldi, C.: Human influence on European winter wind storms such as those of January 2018, Earth Syst. Dynam., 10, 271–286, https://doi.org/10.5194/esd-10-271-2019, 2019.

Vicente-Serrano, S. M., Beguería, S., and López-Moreno, J.I.: A Multiscalar Drought Index Sensitive to Global Warming: The Standardized Precipitation Evapotranspiration Index, J. Climate, 23, 1696-1718, https://doi.org/10.1175/2009JCLI2909.1, 2010.

Vogel, M. M., Zscheischler, J., Wartenburger, R., Dee, D., and Seneviratne, S. I.: Concurrent 2018 hot extremes across Northern Hemisphere due to human-induced climate change, Earth's future, 7, 692– 703, https://doi.org/10.1029/2019EF001189, 2019.

von Bloh, W., Schaphoff, S., Müller, C., Rolinski, S., Waha, K., and Zaehle, S.: Implementing the nitrogen cycle into the dynamic global vegetation, hydrology, and crop growth model LPJmL (version 5.0), Geosci. Model Develop., 11, 2789–2812. https://doi.org/10.5194/gmd-11-2789-2018, 2018.

Wetter3.de (n.d.): Die ganze Welt in Wetterkarte. Retrieved 5 December 2022, from https://www.wetter3.de/index_dt.html

Wild, M.: Global dimming and brightening: A review, J. Geophys. Res., 114, D00D16, https://doi.org/10.1029/2008JD011470, 2009.

Wild, M.: Decadal changes in radiative fluxes at land and ocean surfaces and their relevance for global warming, Wiley Interdisc. Reviews: Climate Change, 7, 91-107, 2016.

Yang, J., and Tian, H.: ISIMIP3b N-deposition input data (v1.0). ISIMIP Repository. https://doi.org/10.48364/ISIMIP.600567, 2020.

Zaitchik, B.F., Omumbo, J., Lowe, R., van Aalst, M., Anderson, L.O., Fischer, E., Norman, C., Robbins, J., Barciela, R., Trtanj, J., von Borries, R., and Luterbacher, J.: Planning for compound hazards during the COVID-19 pandemic: the role of climate information systems. Bull. Americ Meteorol. Soc., 103, E704-E709, 2022.

Zampieri, M., Ceglar, A., Dentener, F., and Toreti, A.: Wheat yield loss attributable to heat waves, drought and water excess at the global, national and subnational scales, Environ. Res. Lett. 12, 064008. https://doi.org/10.1088/1748-9326/aa723b, 2017.

Zscheischler, J., and Fischer, E.M.: The record-breaking compound hot and dry 2018 growing season in Germany, Weather Clim. Extrem., 29, 100270. https://doi.org/10.1016/j.wace.2020.100270, 2020.

Zscheischler, J., Martius, O., Westra, S., Bevacqua, E., Raymond, C., Horton, R. M., van den Hurk, B., AghaKouchak, A., Jézéquel, A., Mahecha, M. D., Maraun, D., Ramos, A. M., Ridder, N. N., Thiery, W. and Vignotto, E.: A typology of compound weather and climate events, Nat. Rev. Earth Environ., 1, 333–347, https://doi.org/10.1038/s43017-020-0060-z, 2020.

Zscheischler, J. and Seneviratne, S.I.: Dependence of drivers affects risks associated with compound events, Sci. Adv. 3, e1700263, 2017.